1 ***Neurochondrin interacts with the SMN protein suggesting a novel mechanism for Spinal Muscular Atrophy***

2 ***pathology.***

3 Luke Thompson, Kim Morrison, Sally Shirran, Catherine Botting, Judith Sleeman, University of St

4 Andrews, School of Biology, BSRC Complex, North Haugh St Andrews, KY16 9ST, UK

Abstract

6 Spinal Muscular Atrophy (SMA) is an inherited neurodegenerative condition caused by reduction

7 in functional Survival Motor Neurones Protein (SMN). SMN has been implicated in transport of

8 mRNA in neural cells for local translation. We previously identified microtubule-dependant mobile

9 vesicles rich in SMN and the splicing factor SmB, a member of the Sm protein family, in neural

10 cells. By comparing the proteome of SmB to that of SmN, a neural-specific Sm protein, we now

11 show that the essential neural protein neurochondrin (NCDN) interacts with Sm proteins and SMN

12 in the context of mobile vesicles in neurites. NCDN has roles in protein localisation in neural cells,

13 and in maintenance of cell polarity. NCDN is required for the correct localisation of SMN,

14 suggesting they may both be required for formation and transport of trafficking vesicles. NCDN

15 provides a potential therapeutic target for SMA together with, or in place of, those targeting SMN

16 expression.

Introduction

18   The inherited neurodegenerative disease, Spinal Muscular Atrophy (SMA) is caused by a

19 reduction in the amount of functional Survival Motor Neuron (SMN) protein (Lefebvre et al. 1995).

20 SMA is the leading genetic cause of infant mortality, affecting 1:6000 live births (Monani 2005).

21 The recently developed therapy, Spinraza/Nusinersin (Biogen) has been shown to increase the

22 level of SMN and improve the symptoms of SMA patients (Passini et al. 2011, Finkel et al. 2016,

23 Corey 2017). Most SMA patients harbour mutations in the SMN1 gene, which produces the

24 majority of total SMN protein in cells. In humans, expression from a variable number of copies of

25 an additional gene, SMN2, can produce some full-length SMN protein (Lefebvre et al. 1995,

26 Lefebvre et al. 1997). The SMN2 gene, unlike SMN1, contains a point mutation in an exon splicing

27 enhancer (Lorson et al. 1999, Lorson, Androphy 2000) resulting in truncation of most of the SMN

28 protein produced by SMN2 through skipping of exon 7. The truncated protein produced by SMN2

29 is less stable than full-length SMN and cannot compensate fully for the loss of SMN1 (Lorson et al.

30 1999, Lorson, Androphy 2000). However, due to the small amounts of full length SMN expressed

31 from the SMN2 gene, the number of gene copies can influence the severity of SMA, with evidence

32 that five copies of SMN2 may be enough to compensate for loss of SMN1 (Campbell et al. 1997,

33 Prior et al. 2004). It is not currently clear how a deficiency of functional SMN leads to the specific

34 symptoms of SMA. In particular, the differing sensitivity of cell types to lowered SMN levels, with

35 motor neurons most severely affected, is difficult to explain as SMN is an essential protein and

36 complete deletion is lethal at the cellular level (Schrank et al. 1997, Hsieh-Li et al. 2000).

37

38 SMN localises to nuclear bodies called gems (Gemini of Cajal bodies (CBs)) (Liu, Dreyfuss

39 1996) as well as in the cytoplasm where it has two well-established cellular roles (Monani 2005,

40 Sleeman 2013, Li et al. 2014, Tisdale, Pellizzoni 2015). The first to be elucidated was a role in the

41 early stages of assembly and maturation of splicing snRNPs (small nuclear ribonucleoproteins).

42 Splicing snRNPs are ribonucleoprotein complexes, essential for pre-mRNA splicing, comprising an

43 snRNA (small nuclear RNA) core and numerous proteins including a heptameric ring containing

44 one copy each of members of the Sm protein family. SMN is part of a cytoplasmic complex, also

45 containing the gemin proteins, required for the addition the Sm proteins as a ring around the

46 snRNA core (Liu et al. 1997, Stark et al. 2001, Li et al. 2014, Tisdale, Pellizzoni 2015). The

47 maturation of snRNPs has been shown to be impaired by a deletion in SMN (Shpargel, Matera

48 2005, Wan et al. 2005, Winkler et al. 2005, Gabanella et al. 2007, Zhang et al. 2008), while

49 alterations to pre-mRNA splicing events, proposed to be a downstream consequence of this

50 impairment, have been observed in several models of SMA (Zhang et al. 2008, Custer et al. 2013,

51 Huo et al. 2014). One of the proposed mechanisms for the cell-type specificity of SMA is that these

52 alterations of pre-mRNA splicing events affect mRNA transcripts that are essential for motor

53 neurons, perhaps preferentially affecting transcripts spliced by the minor spliceosome (Gabanella

54 et al. 2007, Zhang et al. 2008, Boulisfane et al. 2011, Custer et al. 2016, Doktor et al. 2017).

55 Despite promising results in Drosophila models, however, specific transcripts affecting MNs are

56 yet to be conclusively identified (Lotti et al. 2012).

57 The second established cellular role of SMN is in the trafficking of mature mRNA within the

58 cytoplasm, particularly in the axons and neurites of neural cell types. (Rossoll et al. 2002, Rossoll et

59 al. 2003a, Zhang et al. 2003, Zhang et al. 2006a, Todd et al. 2010a, Todd et al. 2010b, Akten et al.

60 2011, Fallini et al. 2011, Peter et al. 2011, Custer et al. 2013, Fallini et al. 2014, Li et al. 2015, Fallini

61 et al. 2016). This is thought to be linked to local translation of mRNA into proteins, an important

62 process for neural cells, in particular motor neurones, due to the length of their axons (Kang,

63 Schuman 1996, Huber et al. 2000, Doyle, Kiebler 2011, Holt, Schuman 2013), making this

64 trafficking role for SMN of particular interest for understanding the cellular pathology of SMA.

SMN co-localises with the mRNA binding proteins HuD, IMP1 and hnRNP R and is involved in the localisation of mRNAs to axons (Rossoll et al. 2003b, Fallini et al. 2011, Akten et al. 2011, Fallini et al. 2014). The cellular structures involved in SMN-dependent mRNA trafficking are currently unclear, being described as granular (Zhang et al. 2003, Peter et al. 2011, Fallini et al. 2014, Akten et al. 2011, Zhang et al. 2006b, Todd et al. 2010b) or vesicular in nature (Custer et al. 2013, Prescott et al. 2014).

Structures containing the SMN and SmB proteins, alongside Coatomer Gamma are trafficked on microtubules (Prescott et al. 2014). Evidence suggesting that SMN/SmB-rich structures are vesicular in nature includes their staining with lipophilic dyes in living neural cells, their vesicular appearance using correlative fluorescence and electron microscopy (Prescott et al. 2014), and the interaction of SMN and the Sm proteins with Coatomer proteins, which are associated with membrane bound vesicles (Peter et al. 2011, Custer et al. 2013, Prescott et al. 2014). We have previously identified an interaction between SmB and dynein cytoplasmic 1 heavy chain 1 (DYNC1H1), a motor protein required for microtubule transport (Prescott et al. 2014), mutation in which can cause a rare, lower extremity dominant SMA (Harms et al. 2010, Harms et al. 2012, Tsurusaki et al. 2012, Niu et al. 2015, Peeters et al. 2015, Punetha et al. 2015, Scoto et al. 2015, Strickland et al. 2015, Ding et al. 2016, Chen et al. 2017). SMN has also been shown to associate with the membranous Golgi complex (Ting et al. 2012), while mutations in the Golgi-related protein BICD2 (bicaudal D homolog 2) causing a form of lower extremity dominant SMA (Neveling et al. 2013, Oates et al. 2013, Peeters et al. 2013, Synofzik et al. 2014, Martinez-Carrera, Wirth 2015, Rossor et al. 2015).

The Sm protein family is implicated in both of the major functions of SMN. The core of splicing snRNPs comprises a heptameric ring of proteins around the snRNA, containing SmB/B', D1, D2, D3 E, F and G (Urlaub et al. 2001). SMN is a vital part of the complex required for the assembly of this Sm protein ring (Liu, Dreyfuss 1996, Fischer et al. 1997, Meister et al. 2001, Meister, Fischer 2002, Pellizzoni et al. 2002, Battle et al. 2006, Fischer et al. 2011). Other members of the Sm protein family have also been identified, beyond the core proteins usually found in splicing snRNPs. Of particular interest in the context of SMA pathology is SmN (encoded by the SNRPN gene), which is expressed in neural tissues (Schmauss et al. 1992) and can replace SmB in the heptameric Sm protein ring (Huntriss et al. 1993). The human SmN protein differs from SmB' by 17 amino acids (UniProt Identifiers P63162 and P14678 respectively), and little is known about its behaviour other than its incorporation into snRNPs, although the SNRPN gene locus is within the

97   paternally imprinted region of the genome critical in Prader-Willi Syndrome (Ozcelik et al. 1992).

98   There is growing appreciation that some Sm proteins may 'moonlight' in functions beyond their

99   presence in splicing snRNPs. In addition to the role of SmB in cytoplasmic trafficking vesicles in

100 human cells, in Drosophila SmB and SmD3 are implicated in mRNA localisation (Gonsalvez et al.

101 2010) and SmD1 has a role in miRNA biogenesis (Xiong et al. 2015). With this in mind, we applied a

102 proteomic approach in the neural cell line SH-SY5Y to search for interactions that could indicate

103 neural specific roles for the SmN protein of relevance for the pathology of SMA.

104   Our proteomic approach led to the identification of a novel interaction between SmN and

105 the essential protein Neurochondrin (NCDN). NCDN is predominantly expressed in neural tissue,

106 where it localises to dendrites, and is involved in the promotion of neural outgrowth (Shinozaki et

107 al. 1997, Shinozaki et al. 1999, Wang et al. 2013, Oku et al. 2013) and the regulation of synaptic

108 plasticity (Dateki et al. 2005, Wang et al. 2009). At a molecular level, NCDN is implicated in the

109 moderation of several signalling pathways in neural cells (Dateki et al. 2005, Francke et al. 2006,

110 Wang et al. 2009, Ward et al. 2009, Wang et al. 2013, Matosin et al. 2015, Pan et al. 2016). NCDN

111 may also have a function in cell polarity maintenance, within dendritic Rab5 positive vesicles (Oku

112 et al. 2013, Guo et al. 2016). Further investigation of NCDN in the context of SMA pathology

113 revealed that it also interacts with SMN. Furthermore, NCDN appears to be required for the

114 correct sub-cellular localisation of SMN. These data suggest that NCDN is involved in a novel,

115 neural-specific role for SMN in the context of mobile cytoplasmic vesicles that also contain a sub-

116 set of the Sm protein family. This has implications both for understanding the cellular pathology of

117 SMA and for the development of additional therapies for the condition.

118 **Results**

119

120 **SmN exhibits similar behaviour to SmB, localising to cytoplasmic vesicles containing SMN**

121

122   In order to determine the interactome of the neural-specific Sm protein, SmN, we first

123 generated constructs to express fluorescent protein-tagged SmN by amplifying the SmN sequence

124 from total RNA from SH-SY5Y cells and cloning it into the pEYFP-C1 and pmCherry-C1vectors. All of

125 the Sm proteins studied so far show a steady-state localisation to nuclear Cajal Bodies (CBs) and

126 speckles. The Sm proteins SmB, SmD1 and SmE have also previously been shown to exhibit a

127 characteristic pathway within the cell on their initial expression, indicative of the snRNP

128 maturation pathway (Sleeman, Lamond 1999), although differences were seen between the Sm

4

129   proteins. To confirm that YFP-SmN localised correctly at steady state to CBs and speckles, and to

130   determine where SmN localised during maturation and incorporation into snRNPs, the plasmid

131   was transiently expressed in SH-SY5Y neuroblastoma cells, with cells fixed and immunostained at

132   24 hour intervals. At 48 and 72 hours after transfection, YFP-SmN predominantly localised to

133   speckles and Cajal bodies (CBs, detected with anti-coilin) identically to endogenous Sm proteins

134   (detected with Y12 antibody), whereas at 24 hours, YFP-SmN localised predominantly diffusely

135   within the cytoplasm, with some accumulation in CBs (Fig 1A, B). This sequential localisation is

136   indistinguishable from that previously observed with YFP-SmB In HeLa and MCF-7 cells, though

137   CBs were not prominent in the majority of SH-SY5Y cells transiently expressing YFP-SmN.

138   Equivalent results were obtained in SH-SY5Y cells transiently expressing mCherry-SmN (Fig S1).

139   Both YFP-SmN and mCherry-SmN are efficiently incorporated into splicing snRNPs, as evidenced by

140   their enrichment from whole-cell lysates using antibodies against the characteristic

141   hypermethylated Cap structure (2,2,7-trimethylaguanosine) found on snRNAs (Fig 1C).

142   To determine whether the similarities between SmN and SmB extend to localisation in

143   vesicles in the cytoplasm (Prescott et al. 2014), SH-SY5Y cells constitutively expressing mCherry-

144   SmN were used for live-cell time-lapse microscopy. Mobile mCherry-SmN foci were observed

145   (movie S1). In common with the SmB vesicles, these stained positive with the lipophilic dye,

146   BODIPY 493, indicating that they are vesicular in nature (Fig 1D). Finally, to confirm that the

147   mCherry-SmN vesicles were similar to those previously identified with SmB, SH-SY5Y cells

148   constitutively expressing mCherry-SmN were transfected with plasmids to express either GFP-SMN

149   or YFP alone. GFP-SMN co-localised with mCherry-SmN in 83% (±11) of SmN-positive vesicles,

150   which is statistically significant when compared to 8.4% (±4.5) of mCherry-SmN vesicles co-

151   localising with YFP alone (Fig 1E, F).

152

153   **Mass Spectrometry reveals the similarities between the interactomes of SmN and SmB**

154

155   As SmN appeared to behave very similarly to SmB in neural cells, it was unclear why neural

156   cells express two almost identical proteins. It was decided to investigate whether SmN and SmB

157   may have differing roles that could be identified by proteomic analysis. Proteins interacting with

158   YFP-SmB and YFP-SmN were affinity purified using GFP-TRAP (Chromotek) from whole-cell lysates

159   of SH-SY5Y cell lines constitutively expressing the tagged proteins, with a cell line expressing YFP

160   alone as a control for non-specific binding to the tag or bead matrix. Immunoblot analysis using

161 antibodies to YFP demonstrated that the enrichment of the tagged proteins was 20X, 23X and 4X

162 for YFP-SmN, YFP-SmB and YFP alone respectively (Fig 2A). The affinity purified material was size

163 separated using SDS-PAGE and analysed by nLC ESI MS/MS mass spectrometry to identify peptides

164 and therefore proteins interacting with YFP-SmB and YFP-SmN. Following removal of likely

165 contaminants identified by their interaction with YFP alone, or their previous identification as

166 common interactors of GFP-TRAP (Trinkle-Mulcahy et al. 2008), UniProt Biological Process and

167 Cellular Component Genome Ontology annotations were used to group identified proteins into

168 categories depending on function. These groups were then used to determine whether there were

169 differences in possible functions between SmN and SmB (Fig 2B). Numerous proteins previously

170 established to interact with Sm proteins were identified including SMN and the gemins as well as

171 the methylosome components PRMT5, MEP50 and pICln, validating our approach (Table S2). The

172 overall proportions of proteins in each category were similar when comparing the interactomes of

173 SmN to SmB, though differences were identified at the level of individual proteins. Of particular

174 interest in the context of SMA were a number of proteins with potential neural specific roles,

175 which were identified in one or both samples. One of these was Neurochondrin (NCDN), a

176 relatively poorly characterised neural protein, which was identified in the YFP-SmN interactome,

177 with 5 unique peptides identified (Fig 2C).

178

179 **Neurochondrin interacts with SmN, SmB and SMN**

180

181 To verify the interaction between Sm proteins and Neurochondrin, a construct expressing

182 NCDN-GFP was generated. Affinity purification of NCDN-GFP from whole cell lysates of SH-SY5Y

183 cells transiently co-expressing NCDN-GFP and mCherry-SmB demonstrated interaction between

184 NCDN-GFP and mCherry-SmB (Fig 3A). To further investigate interactions between NCDN and the

185 Sm proteins neural cells, an SH-SY5Y cell line constitutively expressing NCDN-GFP was established.

186 Affinity purification of NCDN-GFP from whole cell lysates followed by immunoblot analysis using

187 antibodies against endogenous SmN and SmB (Fig 3B) revealed that NCDN-GFP interacts with both

188 SmN and SmB. Furthermore, both endogenous SMN and endogenous βCOP (a coatomer vesicle

189 protein) were also revealed to interact with NCDN-GFP, suggesting that NCDN interacts with the

190 Sm proteins and SMN in the context of cytoplasmic vesicles. Affinity purification of YFP alone from

191 whole cell lysates of an SH-SY5Y cell line constitutively expressing YFP does not result in co-

192 purification of endogenous SMN, SmB or βCOP (Fig 3C). To further investigate the interaction

6

193 between SMN and NCDN observed in Fig 3B, a reciprocal experiment was performed using GFP-

194 Trap to affinity purify GFP-SMN from an SH-SY5Y cell line constitutively expressing GFP-SMN

195 (Clelland et al. 2009). Subsequent immunoblot analysis using antibodies to endogenous NCDN

196 demonstrated that NCDN co-enriched with GFP-SMN (Fig 3D). To determine the probable cellular

197 location for the interaction between SmN/SmB and NCDN plasmids to express either NCDN-GFP or

198 YFP were transiently transfected into SH-SY5Y cells constitutively expressing mCherry-SmN. This

199 revealed that NCDN-GFP, but not YFP alone, accumulates in cytoplasmic vesicles containing

200 mCherry-SmN (Fig3E). Similar results were obtained when NCDN-GFP was transiently expressed in

201 SH-SY5Y cells constitutively expressing mCherry-SmB (Fig S3). To investigate the probable cellular

202 location of interactions between SMN and NCDN, mCherry-SMN was co-expressed with either

203 NCDN-GFP or YFP alone. NCDN-GFP was found in cytoplasmic structures enriched in mCherry-SMN

204 (Fig 3F). These data suggest that NCDN co-localises with both the Sm proteins and SMN in

205 cytoplasmic vesicles, although NCDN-GFP shows an increase diffuse signal compared to the Sm

206 proteins or SMN.

207

208 **NCDN, SMN and Sm protein co-fractionate with coatomer proteins.**

209

210 To further investigate the possibility that the interaction of NCDN with SMN and the Sm

211 proteins occurs within cytoplasmic vesicles, sub-cellular fractionations were performed on both

212 parental SH-SY5Y cells and SH-SY5Y cell lines constitutively expressing NCDN-GFP, YFP-SmB, YFP-

213 SmN or YFP. Sequential centrifugation was used to separate the cells into a nuclear fraction,

214 16,000 RCF and 100,000 RCF cytoplasmic pellets and cytosolic supernatant (de Duve 1971, Lodish

215 et al. 2000, Mohr, Völkl 2001, Andersen et al. 2002). Immunoblotting of these sub-cellular

216 fractions revealed that GFP-NCDN, YFP-SmB and YFP-SmN, were all enriched in the 100,000 RCF

217 pellet, along with endogenous SMN and coatomer proteins (Fig 4). This fraction would be

218 expected to contain membrane-bound structures, such as microsomes and small cytoplasmic

219 vesicles, which would encompass small coatomer type endocytic vesicles (de Duve 1971, Mohr,

220 Völkl 2001, Lodish et al. 2000). Endogenous SmN and SmB were also observed to enrich similarly

221 (Fig S4). NCDN-GFP shows a larger proportion of protein in the remaining cytosolic supernatant

222 when compared to YFP-SmB, YFP-SmN and endogenous SMN, which is in agreement with the sub-

223 cellular localisations observed (Fig 3). This further supports our hypothesis that the interactions

224 between NCDN, SMN and the Sm proteins take place in small cytoplasmic vesicles.

225

NCDN is required for the correct sub-cellular localisation of SMN

227

228   We have previously documented that reduction of SmB expression results in re-localisation

229   of SMN into numerous nuclear structures, probably analogous to gems (Gemini of CBs), and its

230   loss from cytoplasmic structures (Prescott et al. 2014). To investigate the requirement for NCDN in

231   cytoplasmic SMN localisation, an SH-SY5Y cell line constitutively expressing GFP-SMN (Clelland et

232   al. 2009) was transfected with siRNAs targeting NCDN (4 different single siRNAs (Dharmacon) and

233   a pooled sample). A reduction in NCDN expression caused an increase in the number of SMN-

234   positive gems present in the cell nucleus, as did a reduction of SmB expression (Fig 5A, B).

235   Conversely, reduction in SMN expression reduced the number of nuclear gems. The use of non-

236   targeting control (siControl) sequences or positive control siRNAs (targeting Lamin A/C) had no

237   effect on the number of nuclear gems. The reduction in gene expression, assayed by

238   immunoblotting, for each siRNA was typically 40-60% (Fig 5C). This suggests that NCDN is required

239   for the correct sub-localisation of SMN. Of potential relevance for SMA pathology, depletion of

240   either NCDN or SmB causes GFP-SMN to adopt a sub-cellular localisation reminiscent of that

241   shown by GFP-SMNΔ7 (Fig 5), a truncated version of SMN that mimics the product of the SMN2

242   gene and is unable to substitute for full-length SMN in models of SMA (Monani et al. 1999, Monani

243   et al. 2000).

244

SMN is required for the correct sub-cellular localisation of NCDN

246

247   To investigate whether NCDN requires the SMN protein for its localisation to vesicles in

248   neural cells, SH-SY5Y cells were transfected with shRNA constructs previously validated to reduce

249   the expression of SMN by an average of 46%, and carrying a GFP marker to unequivocally identify

250   transfected cells (Clelland et al. 2012). Reduction of SMN reduced the number of cytoplasmic foci

251   containing endogenous NCDN (Fig 6A, B). A reduction in the number of nuclear gems (identified

252   with SMN) was also observed, confirming that the shRNA was reducing SMN expression (Fig 6A, C).

253   This, together with data in Figure 5, suggests that NCDN and SMN are mutually dependant for

254   their incorporation into cytoplasmic structures, raising the possibility that the lowered levels of

255   SMN seen in SMA could compromise NCDN function.

256

NCDN does not co-purify with splicing snRNPs, suggesting it is not involved in snRNP assembly

258

259   To investigate whether the interaction between NCDN and SMN could reflect a previously

260   unidentified role for NCDN in snRNP assembly, splicing snRNPs were affinity purified from whole

261   cells lysates of SH-SY5Y cells constitutively expressing NCDN-GFP using agarose beads coupled to

262   antibodies against the characteristic tri-methyl guanosine Cap of snRNAs (TMG beads, Millipore)

263   (Fig 7). Endogenous Sm proteins showed strong enrichment in the affinity purified snRNP samples,

264   as expected for a core snRNP protein. Endogenous SMN was also co-enriched, demonstrating that

265   the experimental conditions were suitable to identify proteins important for snRNP assembly.

266   NCDN-GFP did not co-purify with splicing snRNPs, suggesting that NCDN is not involved in snRNP

267   assembly or processing. This raises the intriguing possibility that the interaction between SMN and

268   NCDN reflects a novel, snRNP-independent role for SMN.

269

SMN interacts with Rab5 in SH-SY5Y cells and co-localises with a sub-set of Rab5 vesicles.

271

272   Recent studies have found that SMA may cause endocytic defects, especially in synaptic

273   vesicle recycling in animal models (Dimitriadi et al. 2016). Several SMA-protective disease modifier

274   genes, such as Plastin 3, Coronin 1C, and Neurocalcin Delta, are also associated with endocytosis

275   (Oprea et al. 2008, Hosseinibarkooie et al. 2016, Riessland et al. 2017). However, other endocytic

276   structures within the cell have not been investigated. Rab5 is a marker of early endosomes and

277   endocytic vesicles, as well as being a regulator of these trafficking pathways (Bucci et al. 1992).

278   NCDN and Rab5 have previously been shown to interact, while both Rab5 and NCDN both have

279   roles in dendrite morphogenesis and cell polarity (Satoh et al. 2008, Oku et al. 2013, Guo et al.

280   2016).

281   As we had previously shown that SMN and NCDN co-localise in vesicles, we hypothesised

282   that some of the SMN-rich vesicles could be Rab5 vesicles. SH-SY5Y cells were co-transfected with

283   plasmids to express mRFP-Rab5 (Vonderheit, Helenius 2005) together with GFP-SMN, NCDN-GFP

284   or YFP. mRFP-Rab5 was affinity-purified from whole cell lysates from each co-transfection using

285   RFP-TRAP (Chromotek). Subsequent immunoblotting revealed co-purification of GFP-SMN and

286   NCDN-GFP, but not YFP alone, with mRFP-Rab5 (Fig 8A). Furthermore, endogenous SMN also co-

287 purified with mRFP-Rab5. In parallel experiments, co-localisation of mRFP-Rab5 with GFP-SMN and

288 NCDN was investigated (Fig 8B, C). In accordance with previous publications, Rab5 showed partial

289 co-localisation with NCDN-GFP in cytoplasmic structures (arrows in Fig 8C) (Oku et al. 2013). GFP-

290 SMN showed a similar degree of co-localisation with mRFP-Rab5, also in cytoplasmic structures,

291 while there was minimal co-localisation between YFP and mRFP-Rab5. Taken together with the

292 data in Figure 7 above this suggests that NCDN and SMN co-localise in the context of Rab5

293 vesicles, independently of snRNP assembly.

294

295 **Discussion**

296

297   The genetic cause of SMA has been known since 1995 (Lefebvre et al. 1995), but there is

298 still little available in the way of treatment. Spinraza/Nusinersin is now available to treat SMA by

299 correcting the defective splicing of the SMN2 transcript to promote production of full-length SMN

300 protein. However, this is not a complete cure and requires regular maintenance doses through

301 intrathecal injection. Additionally, little has been done to investigate potential symptoms that

302 could arise later in life or in other tissues and organs in patients treated with Spinraza. Additional

303 treatment options for SMA are still needed, for use in addition to Spinraza, or in place of it for

304 patients for whom it is not suitable, including those with more rare forms of SMA in which SMN is

305 not mutated.

306   A significant reason for the lack of treatment options for SMA is uncertainty about the

307 cellular roles of SMN, which appear to be numerous. In particular, it is not clear why motor

308 neurones are so exquisitely sensitive to reduced levels of SMN when the key roles of the protein

309 appear to be in pathways required in all cell types. By comparing the interactomes of two very

310 similar members of Sm protein family, SmB and the neural-specific SmN, we have uncovered an

311 interaction between SMN and the essential neural protein NCDN, which may open novel avenues

312 for therapy development.

313 **The neural-specific Sm protein, SmN, behaves similarly to SmB, but shows subtle differences at**

314 **the interactome level that may indicate alternative roles.**

315

316   Differences between members of the Sm protein family have not been systematically

317 investigated, although non-splicing roles have been proposed for SmB and SmD3 in mRNA

10

318 localisation and for SmD1 in miRNA biogenesis in Drosophila (Gonsalvez et al. 2010, Xiong et al.

319 2015). As SmB and SmN are thought to perform the same primary function in snRNPs (Huntriss et

320 al. 1993), it is currently unknown why SmN is expressed in neural tissues as well as, or instead of,

321 SmB. Current research has suggested that the expression of SmN may cause tissue specific

322 alternative splicing of pre-mRNA transcripts (Lee et al. 2014). However, an alternative, but

323 complimentary hypothesis is that SmN may be adapted for secondary, neural specific roles. We

324 demonstrate here that SmN localises identically to SmB during snRNP maturation and at steady-

325 state where both localise to vesicles containing SMN in the cytoplasm and neurites of SH-SY5Y

326 cells in addition to their canonical localisation to nuclear CBs and speckles. Our parallel proteomic

327 study used SH-SY5Y neural cell lines constitutively expressing YFP-SmN and YFP-SmB to investigate

328 difference between the interactomes of these two, very similar, proteins. YFP-SmN has a proline

329 rich C-terminal tail that YFP-SmB lacks, although a similar sequence is present in SmB' (Mourão et

330 al. 2016), an alternatively-spliced product of the SNRPB gene, which encodes SmB. Several

331 proteins were identified in the SmN interactome but not the SmB interactome such as nuclear

332 receptor co-activator 6 interacting protein (UniProt Q96RS0), and 7SK snRNA methylphosphate

333 capping enzyme (UniProt Q7L2J0), both of which are associated with snRNA capping (Jeronimo et

334 al. 2007, Hausmann et al. 2008). Additionally, RNA-binding protein 40 (UniProt Q96LT9) was

335 uniquely identified within the SmN interactome, and is involved in the minor spliceosome

336 (Benecke et al. 2005). This suggests that some of these proteins may interact preferentially with

337 SmN, perhaps mediated by amino acid changes within the proline-rich tail. However, further

338 validation and additional experimentation would be required to confirm these differences in

339 interactome between SmN and SmB and to investigate specific functions for the distinct Sm

340 protein family members.

341

342 **NCDN interacts with SMN, SmB and SmN and co-localises with them in vesicles, suggesting a**

343 **novel cellular role for SMN.**

344

345   Previous research into neural-specific functions for SMN has identified several new

346 protein-protein interactions involving SMN. These novel SMN partners have, in the main, been

347 RNA binding proteins (Rossoll et al. 2003b, Fallini et al. 2011, Akten et al. 2011, Fallini et al. 2014).

348 There is growing appreciation that SMN-mediated transport may be of particular importance in

349 neural cells and involve COP1-type vesicles transported by Dynein and containing SmB (Peter et al.

350   2011, Custer et al. 2013, Prescott et al. 2014, Li et al. 2015). The nature and content of these

351   vesicles is not clear but they are likely to be of significance for the cell-type bias of SMA symptoms,

352   as they are present predominantly in neural cells (Rossoll et al. 2003a, Zhang et al. 2003, Zhang et

353   al. 2006a, Todd et al. 2010a, Todd et al. 2010b, Akten et al. 2011, Fallini et al. 2011, Peter et al.

354   2011, Custer et al. 2013, Fallini et al. 2014, Prescott et al. 2014, Li et al. 2015, Fallini et al. 2016).

355   The SmN/SmB interactome screen presented here suggests a large number of non-snRNP proteins

356   as potential cellular partners for the Sm proteins.

357   We chose to investigate the neural protein NCDN further, as it has characteristics that may

358   be of relevance for SMA. NCDN is predominantly expressed in neural tissue, and little is known

359   about its structure or function, as it shares little sequence homology with other eukaryotic

360   proteins (Shinozaki et al, 1997). Though characterised relatively poorly, it is associated with

361   dendrite morphogenesis and localises to Rab5 vesicles involved in the maintenance of cell polarity

362   (Oku et al. 2013, Guo et al. 2016), NCDN has also been demonstrated to regulate localisation of

363   signalling proteins such as P-Rex 1 (Pan et al. 2016), suggesting that it, in common with SMN, has a

364   role in intra-cellular trafficking. These neural-specific and trafficking roles suggest that further

365   analysis of the interaction between NCDN and the Sm proteins may help to better understand the

366   molecular mechanisms of pathogenesis in SMA.

367   Reciprocal affinity-purification of GFP-tagged and endogenous NCDN and Sm proteins (Fig

368   3A, B) validated the interaction detected in the interactome analysis. Although originally identified

369   as a protein interacting with SmN but not SmB, further investigation indicates that NCDN is, in

370   fact, capable of interacting with both of these Sm proteins. Of much greater interest, however, is

371   the interaction documented between NCDN and SMN, which appears more robust than that

372   between NCDN and the Sm proteins (Fig 3B, E). Furthermore, NCDN is excluded from the cell

373   nucleus and localises with SMN and the Sm proteins in mobile vesicles in the neurites of SH-SY5Y

374   cells (Fig 3D, F) suggesting that it shares cytoplasmic, rather than nuclear, roles with SMN. The

375   truncated protein SMNΔ7, which can't fully substitute for FL-SMN, is largely restricted to the

376   nucleus (Renvoisé et al. 2006, Sleigh et al. 2011). While it can't yet be ruled out that SMNΔ7 lacks

377   the capability to substitute for FL-SMN in nuclear roles, this suggests that cytoplasmic roles of

378   SMN are key to SMA pathology. NCDN was not co-purified with splicing snRNPs, under conditions

379   that showed a clear enrichment of SMN in the snRNP fraction. This suggests that the interaction

380   between NCDN, SMN and the Sm proteins is not related to snRNP assembly.

381

12

Potential consequences of NCDN mis-localisation associated with SMN reduction

We have identified co-localisation of both SMN and NCDN with a sub-set of Rab5 vesicles. Since NCDN is also found in a sub-set of SMN-positive cytoplasmic structures, it is highly likely that these are Rab5 vesicles. It is possible that the protein-protein interactions between NCDN and SMN occur elsewhere in the cytoplasm as both proteins also show a diffuse cytosolic pool, but the decrease seen in cytoplasmic structures containing NCDN following SMN depletion suggest that cellular pathways requiring NCDN-containing vesicles may be compromised in SMA.

At present, the precise roles of NCDN are not fully understood, although it has been implicated in dendrite morphogenesis, neural outgrowth, synaptic plasticity regulation, and moderation of signalling pathways in neural cells (Shinozaki et al. 1997, Shinozaki et al. 1999, Ohoka et al, 2001, Dateki et al. 2005, Francke et al. 2006, Wang et al. 2009, Ward et al. 2009, Oku et al. 2013, Wang et al. 2013, Matosin et al. 2015, Pan et al. 2016). NCDN has also previously been shown to localise to Rab5 vesicles within dendrites (Oku et al. 2013). These dendritic Rab5 vesicles have been found have an important role in dendrite morphogenesis and somatodendritic polarity (Satoh et al. 2008, Guo et al. 2016). As we have now demonstrated that SMN localises to a sub-set of Rab5 vesicles, likely in association with NCDN, SMN may also be implicated in cell polarity, with an insufficiency of SMN causing problems with both establishment and maintenance of polarity. These would be particularly vital in such elongated cells as motor neurons and may be mediated through trafficking of mRNAs or proteins. Further work will be required to investigate defects in cell polarity as a pathogenic mechanism in SMA and their possible link to NCDN.

NCDN as a novel therapeutic target in SMA.

SMN has now been linked to several functions other than its canonical role in snRNP assembly. While reduction in the cell's capacity for snRNP assembly caused by lowered SMN may cause splicing defects, the key transcripts preferentially affecting motor neurones are still to be identified. SMN has an established role in the trafficking of mature mRNAs destined for localised translation. The nature of the structures involved in this role is not completely clear, however, with different authors describing the structures as vesicular or granular. Reduction of SMN has also been linked with endosomal defects, suggestive of the importance of SMN for vesicular transport. Here we provide further evidence for the presence of SMN in, or associated with,

13

413 vesicles and identify the essential neural protein, NCDN as a potential target for therapy

414 development in SMA. Further work will be required to establish which roles of NCDN also involve

415 SMN, however the co-dependence of SMN and NCDN in cytoplasmic vesicles suggests that

416 depletion of SMN, as seen in the majority of SMA patients, may affect NCDN localisation and/or

417 function. Manipulation of the expression or function of NCDN may, therefore, have potential as

418 an SMN-independent target for the development of novel therapies for SMA.

419

420 **Materials and Methods**

421 *Plasmid constructs*

422 pEGFP-SMN, pEYFP-SmB and mCherry-SmB have been described previously (Sleeman, Lamond

423 1999, Sleeman et al. 2001, Clelland et al. 2009). pEYFP-SmN and pmCherry-SmN were generated

424 by PCR amplification and sub-cloning cDNA of human SmN from SH-SY5Y cells into pEYFP-C1 and

425 pmCherry-C1 respectively, using SNRPNEcoRI forward primer:

426 TAGAATTCCATGACTGTTGGCAAGAGTAGC, and SNRPNBamHI reverse primer:

427 TAGGATCCCTGAGATGGATCAACAGTATG. pmCherry-SMN was generated by PCR amplification sub-

428 cloning the sequence from the pEGFP-SMN plasmid into pmCherry-C1 using an SMNEcoRI Forward

429 primer: GCGGAATTCTATGGCGATGAGC and SMNBamHI Reverse Primer:

430 GCAGGATCCTTAATTTAAGGAATGTGA. To generate pEGFP-NCDN, NCDN cDNA from SH-SY5Y cells

431 was PCR amplified and sub-cloned into a pEGFP-N3 plasmid using NCDNEcoRI forward primer:

432 GCGGAATTCATGGCCTCGGATTGCG and NCDNSalI reverse primer: GCTGCTGACGGGCTCTGACAGGC.

433 All cDNAs were amplified using GoTaq G2 (Promega) and the PCR products restriction digested

434 using EcoRI and either BamHI or SalI (Promega), before ligation with T4 DNA ligase (Thermo

435 Scientific). mRFP-Rab5 was a gift from Ari Helenius (Vonderheit, Helenius 2005).

436 *Cell lines and cell culture*

437 SH-SY5Y cells were from ATCC. Cells were cultured in DMEM with 10% FBS at 37°C, 5% CO_2.

438 Transfections were carried out using Effectene (Qiagen) according to the manufacturer's

439 instructions. Stable SH-SY5Y cell lines expressing mCherry–SmB and GFP–SMN have been

440 described previously (Clelland et al. 2009, Prescott et al. 2014). SH-SY5Y cell lines stably expressing

441 YFP-SmN, YFP-SmB, YFP, mCherry-SmN and NCDN-GFP were derived by clonal isolation following

442 selection with 200 µg/ml G418 (Roche) following transfection.

14

443   *Immunostaining, microscopy and image analysis*

444   Cell fixing and immunostaining were both carried out as described previously (Sleeman et al.

445   2003). Live cell and fixed cell microscopy and image processing were carried out as described

446   previously (Prescott et al. 2014). BODIPY-493 (Life Technologies) was added to culture medium at

447   2 µg/ml overnight. Antibodies used for immunostaining were Mouse monoclonal Y12 anti-Smith

448   (SmB) (Abcam ab3138, 1:20), Rabbit polyclonal 204-10 (anti-Coilin) (a gift from A. I. Lamond

449   (Bohmann et al. 1995), 1:500), Mouse monoclonal anti-SMN (BD Transduction 610646, 1:50) and

450   Rabbit polyclonal anti-NCDN (Proteintech 13187-1-AP, 1:50). Overlays of images were made using

451   Adobe Photoshop CS5 (Adobe). Co-localisation images were generated using Volocity 6.3

452   (PerkinElmer), using automatic thresholds on non-deconvolved images. Co-localisation values of

453   0.05 or less were excluded as this was the maximum co-localisation value observed between

454   mCherry signal and YFP signal in neurites expressing YFP as a control together with mCherry-

455   tagged proteins of interest. Deconvolution was also performed using Volocity 6.3, with between

456   15 and 25 iterations of deconvolution.

457

458   *Statistical Analysis, and generation of graphs*

459   Data was processed using Microsoft Excel (Microsoft) to produce ratios, proportions and

460   percentages. Bar charts, Box and Whisker plots were then generated using Prism 6 (GraphPad)

461   from the processed data. Statistical analysis was also performed using Prism 6, with multiple

462   comparisons to determine statistical difference between specific sets of data. Tukey post-tests

463   were used to identify outliers in Anova statistical analysis.

464

465   *Preparation of cell lysates and immunoblotting*

466   Cells were grown in 10cm diameter dishes, before being detached with trypsin and collected by

467   centrifugation at 180 RCF for 5 minutes. The cell pellet was washed 3 times in PBS before lysis in

468   100µl of ice cold lysis buffer per dish (50 mM Tris-HCl pH 7.5; 0.5 M NaCl; 1% (v/v) Nonidet P-40;

469   1% (w/v) sodium deoxycholate; 0.1% (w/v) SDS; 2 mM EDTA plus cOmplete mini EDTA-free

470   protease inhibitor cocktail (Roche, one tablet per 10 ml)), followed by homogenisation by

471   sonication. Isolation of YFP/GFP and mCherry/mRFP- tagged proteins was carried out as described

472   previously with GFP- or RFP-Trap (Chromotek) (Prescott et al. 2014). Lysates were electrophoresed

473   on a 10% SDS-polyacrylamide gel and transferred to nitro-cellulose (Hybond-C+ or Protran

474   premium 0.2µm, both GE Healthcare) membranes for immunoblotting. Antibodies used were rat

475   monoclonal anti-RFP (Chromotek 5F8, 1 : 500); goat polyclonal anti-γCOP (Santa Cruz sc-14167,

15

476 1：250), rabbit polyclonal anti-GFP (Abcam ab290, 1:2000), rabbit polyclonal anti-SNRPN (SmN)

477 (Proteintech 11070-1-AP, 1:800), mouse monoclonal Y12 anti-Smith (SmB) (Abcam ab3138,

478 1:100), rabbit polyclonal anti-SMN (Santa Cruz sc-15320, 1:500), mouse monoclonal anti-SMN (BD

479 Transduction labs 610646, 1:500), rabbit polyclonal anti-COPB1 (CUSAB CSB-PA005783LA01HU,

480 1:500), mouse monoclonal anti-Lamin A/C (Santa Cruz sc-7292, 1:500), rabbit polyclonal anti-

481 NCDN (Proteintech 13187-1-AP, 1:500), mouse Monoclonal anti-tubulin (Sigma Aldrich, 1:500) and

482 rabbit polyclonal anti-Histone H3 (Proteintech 17168-1-AP, 1:300). Secondary antibodies were

483 goat anti-rabbit Dylight 700 (Thermo Scientific 35569, 1:15,000) or goat anti-mouse Dylight 800

484 (Thermo Scientific SA5-10176, 1:15,000). Alternatively, goat anti-mouse IRDye 800CW (Li-Cor 925-

485 32210, 1:25,000) and goat anti-rabbit IRDye 680RD (Li-Cor 925-68071, 1:25,000) were used. Goat

486 anti-Rat Dylight 800 (Thermo Scientific, SA5-10024) antibody was used to visualise the rat

487 monoclonal anti-RFP antibody at a concentration of 1:15,000. Donkey anti-goat IRDye 800CW

488 (Licor, 925-32214) was used at a concentration of 1:25,000 to detect goat polyclonal anti-γCOP.

489 Donkey anti-rabbit conjugated to horseradish peroxidase (HRP) (Pierce, 31460, 1:15,000) was used

490 to identify endogenous NCDN in figure 3D. Detection of antibodies conjugated to fluorophores

491 was carried out with an Odessey CLx using Image Studio (both Li-cor). Band quantification was also

492 performed using Image Studio. Detection of antibodies conjugated to peroxidase was performed

493 using ECL Western Blotting Substrate (Pierce) and developed with Hyperfilm (Amersham), using a

494 Kodak X-OMAT 1000 developer, after 30-45 minutes exposure.

495 *Immunoprecipitation of intact snRNPs*

496 To immunoprecipitate intact snRNPS, whole cell lysates were incubated with anti-2,2,7-

497 trimethylguanosine conjugated to agarose beads (Millipore NA02A), with Sepharose 4B beads

498 (Sigma Aldrich) as a control. 40 ng of pre-cleared lysate and unbound protein were separated by

499 SDS-PAGE alongside material precipitated with Sepharose control beads and TMG antibody beads.

500 Subsequent detection was carried out using rabbit anti-GFP (1:2000, Abcam), rat mAb anti-RFP

501 (1:500, Chromotek), mouse monoclonal anti-SMN (1:500, BD Transduction labs) and rabbit

502 polyclonal anti-SNRPN (1:800, Proteintech).

503 *Preparations and analysis of Mass Spectrometry samples*

504 SH-SY5Y cells constitutively expressing either YFP, YFP-SmN or YFP-SmB were lysed in co-

505 immunoprecipitation buffer (10mM Tris pH7.5, 150mM NaCl, 0.5mM EDTA, 0.5% NP40, 1

506 cOmplete EDTA-free protease inhibitor tablet (Roche) per 10ml), followed by affinity purification

507 of the tagged proteins with GFP-Trap as above. 5μl of the affinity isolated material, alongside

16

508   precleared lysate and unbound lysate was transferred to nitrocellulose membrane (as above) and

509   immunodetected using Rabbit anti-GFP (Abcam) to confirm efficient immunoprecipitation.

510   Samples were then electrophoresed on a NuPAGE 4-12% Bis-Tris Acrylamide gel (Novex NP0321),

511   Coomassie stained using SimplyBlue SafeStain (Invitrogen), gel chunks excised and analysed by the

512   Mass Spectrometry and Proteomics Facility at the University of St Andrews.

513   The gel chunks were cut into 1 mm cubes. These were then subjected to in-gel digestion, using a

514   ProGest Investigator in-gel digestion robot (Digilab) using standard protocols (Shevchenko et al.

515   1996). Briefly, the gel cubes were destained by washing with MeCN and subjected to reduction

516   with DTT and alkylation with IAA before digestion overnight with trypsin at 37°C. The peptides

517   were extracted with 10% formic acid, and the volume reduced to ~20ul by concentration in a

518   speedvac (ThermoSavant).

519   The peptides were then injected onto an Acclaim PepMap 100 C18 trap and an Acclaim PepMap

520   RSLC C18 column (ThermoFisher Scientific), using a nanoLC Ultra 2D plus loading pump and

521   nanoLC as-2 autosampler (Eksigent). The peptides were eluted with a gradient of increasing

522   acetonitrile, containing 0.1 % formic acid (2-20% acetonitrile in 90 min, 20-40% in a further 30 min,

523   followed by 98% acetonitrile to clean the column, before re-equilibration to 2% acetonitrile). The

524   eluate was sprayed directly into a TripleTOF 5600 electrospray tandem mass spectrometer (Sciex,

525   Foster City, CA) and analysed in Information Dependent Acquisition (IDA) mode, performing 250

526   msec of MS followed by 100 msec MS/MS analyses on the 20 most intense peaks seen by MS. The

527   MS/MS data file generated via the 'Create mgf file' script in PeakView (Sciex) was analysed using

528   the Mascot search algorithm (Matrix Science), against the NCBInr database (Oct 2014) restricting

529   the search to Homo sapiens (284,317 sequences), trypsin as the cleavage enzyme and

530   carbamidomethyl as a fixed modification of cysteines and methionine oxidation as a variable

531   modification. The peptide mass tolerance was set to ± 0.05 Da and the MSMS mass tolerance to ±

532   0.1 Da.

533   Scaffold viewer (version Scaffold_4.5.1, Proteome Software) was used to validate MS/MS based

534   peptide and protein identifications. Peptide identifications were accepted if they could be

535   established at greater than 95.0% probability by the Peptide Prophet algorithm (Keller et al. 2002).

536   Protein identifications were accepted if they could be established at greater than 99.0%

537   probability and contained at least 2 identified peptides. Protein probabilities were assigned by the

538   Protein Prophet algorithm (Nesvizhskii et al. 2003). Proteins that contained similar peptides and

17

539   could not be differentiated based on MS/MS analysis alone were grouped to satisfy the principles

540   of parsimony.

541   Identified proteins affinity purified alongside YFP-SmB or YFP-SmN were discounted if they were

542   additionally identified as being affinity purified with YFP, or if they were present within the

543   Sepharose bead proteome (Trinkle-Mulcahy et al. 2008).

544   *RNAi assays*

545   Reduction of protein expression using siRNA was achieved by transfecting the appropriate cell

546   lines with siRNAs (Dharmacon) using Viromer Green (Lipocalyx GmbH) according to the

547   manufacturer's instructions. Cells were lysed for assay by immunoblotting, or fixed with

548   paraformaldehyde for fluorescence microscopy, 48 hours after transfection. Sequences used were

549   SMN: CAGUGGAAAGUUGGGGACA; SmB, a mixture of CCCACAAGGAAGAGGUACU,

550   GCAUAUUGAUUACAGGAUG, CCGUAAGGCUGUACAUAGU, CAAUGACAGUAGAGGGACC; NCDN,

551   individually and a mixture of NCDN 18 GUUCAUUGGUGACGAGAAA, NCDN 19

552   AGACCUCAUCCUUGCGUAA, NCDN 20 AGGCCAAGAAUGACAGCGA, NCDN 21

553   GGCCAUUGAUAUCGCAGUU; negative control (siControl) targeting luciferase,

554   UAAGGCUAUGAAGAGAUAC; positive control targeting Lamin A/C, GGUGGUGACGAUCUGGGCU;

555   SiGlo Cyclophillin B to determine transfection efficiency, GGAAAGACUGUUCCAAAAA. Lysates

556   were electrophoresed on an SDS-PAGE gel, transferred to nitrocellulose membrane, and

557   immunodetected with antibodies to the above proteins. Band signal intensity determined with

558   ImageStudio (Li-Cor), and the values were normalised to Tubulin.Reduction of protein expression

559   using shRNA was achieved by transfecting SH-SH5Y cell lines with pSUPER-GFP.Neo plasmids

560   (Oligoengine) expressing shRNA to SMN and Cyclophilin B, which have been described previously

561   (Clelland et al. 2012) using Effectene (QIAGEN).

562   *Fractionation*

563   Cells were pelleted from the appropriate cell line, and incubated in Buffer A (10mM HEPES pH7.9,

564   1.5mM $MgCl_2$, 10mM KCl, 0.5mM DTT, 1 cOmplete EDTA-free protease inhibitor tablet per 10ml)

565   for 5 minutes, before being Dounce homogenised 25 times using the tight pestle to disrupt the

566   plasma membrane. This was then centrifuged at 300 RCF for 5 minutes to pellet the nuclei. The

567   supernatant was removed, recentrifuged at 300 RCF to further remove nuclei, before the

568   supernatant was centrifuged at 16,100 RCF for 30 minutes using a refrigerated 5415R Centrifuge

569   (Eppendorf). The nuclei were resuspended in Buffer S1 (250mM Sucrose, 10mM $MgCl_2$), before

570   this was layered over with Buffer S3 (880mM Sucrose, 0.5mM $MgCl_2$). The nuclear pellet was then

571 centrifuged at 2800 RCF for 10 minutes to wash and pellet the nuclei. The supernatant from the

572 16,100 RCF centrifugation was further centrifuged at 100,000 RCF using an Optima Max-XP

573 ultracentrifuge with a TLA-110 Rotor (Beckman-Coulter) for 60 minutes. The supernatant was

574 removed and kept. The 16,100 and 100,000 RCF pellets were washed in Buffer A and centrifuged

575 at 16,100 RCF for 30 minutes or 100,000 RCF for 1 hour respectively. Each pellet was then

576 resuspended in lysis buffer (see above). To confirm efficient separation of cytoplasmic fractions

577 from the nuclear fractions, Mouse anti-tubulin (Sigma Aldrich, 1:500) and Rabbit polyclonal anti-

578 Histone H3 (Proteintech, 1:300) antibodies were used.

583 ***Competing Interests***

584 The use of NCDN as a modulator compound for developing SMA therapies is the subject of patent

585 application GB1710433.2 filed 29 June 2017 at the UK IPO.

591 **Author contributions:**

592 LWT designed experiments, generated reagents, produced and analysed data, generated the

593 figures and helped to prepare and edit the manuscript. KM acquired and analysed data. SS and CB

594 processed the MS samples, produced the MS/MS data set and assisted with analysis. JES came up

595 with the original concept, designed experiments, analysed data and prepared and edited the

596 manuscript.

597

References

Akten, B., Kye, M.J., Hao, L.T., Wertz, M.H., Singh, S., Nie, D., Huang, J., Merianda, T.T., Twiss, J.L., Beattie, C.E., Steen, J.A.J. and Sahin, M. (2011). Interaction of survival of motor neuron (SMN) and HuD proteins with mRNA cpg15 rescues motor neuron axonal deficits. *Proceedings of the National Academy of Sciences*. 108(25), 10337-10342.

Andersen, J.S., Lyon, C.E., Fox, A.H., Leung, A.K.L., Lam, Y.W., Steen, H., Mann, M. and Lamond, A.I. (2002). Directed Proteomic Analysis of the Human Nucleolus. *Current Biology*. 12(1), 1-11.

Battle, D.J., Kasim, M., Yong, J., Lotti, F., Lau, C.-., Mouaikel, J., Zhang, Z., Han, K., Wan, L. and Dreyfuss, G. (2006). The SMN Complex: An Assembly Machine for RNPs. *Cold Spring Harbor Symposia on Quantitative Biology*. 71, 313-320.

Bedford, M.T., Reed, R. and Leder, P. (1998). WW domain-mediated interactions reveal a spliceosome-associated protein that binds a third class of proline-rich motif: The proline glycine and methionine-rich motif. *Proceedings of the National Academy of Sciences*. 95(18), 10602-10607.

Bedford, M.T., Sarbassova, D., Xu, J., Leder, P. and Yaffe, M.B. (2000). A Novel Pro-Arg Motif Recognized by WW Domains. *Journal of Biological Chemistry*. 275(14), 10359-10369.

Benecke, H., Lührmann, R. and Will, C.L. (2005). The U11/U12 snRNP 65K protein acts as a molecular bridge, binding the U12 snRNA and U11-59K protein. *Embo J*. 24(17), 3057.

Bohmann, K., Ferreira, J.A. and Lamond, A.I. (1995). Mutational analysis of p80 coilin indicates a functional interaction between coiled bodies and the nucleolus. *The Journal of Cell Biology*. 131(4), 817-831.

Boulisfane, N., Choleza, M., Rage, F., Neel, H., Soret, J. and Bordonné, R. (2011). Impaired minor tri-snRNP assembly generates differential splicing defects of U12-type introns in lymphoblasts derived from a type I SMA patient. *Human Molecular Genetics*. 20(4), 641-648.

Bucci, C., Parton, R.G., Mather, I.H., Stunnenberg, H., Simons, K., Hoflack, B. and Zerial, M. (1992). The small GTPase rab5 functions as a regulatory factor in the early endocytic pathway. *Cell*. 70(5), 715-728.

Campbell, L., Potter, A., Ignatius, J., Dubowitz, V. and Davies, K. (1997). Genomic Variation and Gene Conversion in Spinal Muscular Atrophy: Implications for Disease Process and Clinical Phenotype. *The American Journal of Human Genetics*. 61(1), 40-50.

Chen, Y., Xu, Y., Li, G., Li, N., Yu, T., Yao, R., Wang, X., Shen, Y. and Wang, J. (2017). Exome Sequencing Identifies De Novo DYNC1H1 Mutations Associated With Distal Spinal Muscular Atrophy and Malformations of Cortical Development. *J Child Neurol*. 32(4), 379-386.

Clelland, A.K., Kinnear, N.P., Oram, L., Burza, J. and Sleeman, J.E. (2009). The SMN Protein is a Key Regulator of Nuclear Architecture in Differentiating Neuroblastoma Cells. *Traffic*. 10(11), 1585-1598.

Clelland, A.K., Bales, A.B.E. and Sleeman, J.E. (2012). Changes in intranuclear mobility of mature snRNPs provide a mechanism for splicing defects in spinal muscular atrophy. *Journal of Cell Science*. 125(11), 2626-2637.

Corey, D.R. (2017). Nusinersen, an antisense oligonucleotide drug for spinal muscular atrophy. *Nature Neuroscience*. 20(4), 497-499.

635   Custer, S.K., Gilson, T.D., Li, H., Todd, A.G., Astroski, J.W., Lin, H., Liu, Y. and Androphy, E.J. (2016). Altered
636   mRNA Splicing in SMN-Depleted Motor Neuron-Like Cells. *Plos One*. 11(10), e0163954.

637   Custer, S.K., Todd, A.G., Singh, N.N. and Androphy, E.J. (2013). Dilysine motifs in exon 2b of SMN protein
638   mediate binding to the COPI vesicle protein a-COP and neurite outgrowth in a cell culture model of spinal
639   muscular atrophy. *Human Molecular Genetics*. 22(20), 4043-4052.

640   Dateki, M., Horii, T., Kasuya, Y., Mochizuki, R., Nagao, Y., Ishida, J., Sugiyama, F., Tanimoto, K., Yagami, K.,
641   Imai, H. and Fukamizu, A. (2005). Neurochondrin Negatively Regulates CaMKII Phosphorylation, and
642   Nervous System-specific Gene Disruption Results in Epileptic Seizure. *Journal of Biological Chemistry*.
643   280(21), 20503-20508.

644   de Duve, C. (1971). TISSUE FRACTION-PAST AND PRESENT. *The Journal of Cell Biology*. 50(1), 20d-55d.

645   Dimitriadi, M., Derdowski, A., Kalloo, G., Maginnis, M.S., O'Hern, P., Bliska, B., Sorkaç, A., Nguyen, K.C.Q.,
646   Cook, S.J., Poulogiannis, G., Atwood, W.J., Hall, D.H. and Hart, A.C. (2016). Decreased function of survival
647   motor neuron protein impairs endocytic pathways. *Proceedings of the National Academy of Sciences*.
648   113(30), E4377-E4386.

649   Ding, D., Chen, Z., Li, K., Long, Z., Ye, W., Tang, Z., Xia, K., Qiu, R., Tang, B. and Jiang, H. (2016). Identification
650   of a de novo DYNC1H1 mutation via WES according to published guidelines. *Scientific Reports*. 6, 20423.

651   Doktor, T.K., Hua, Y., Andersen, H.S., Brøner, S., Liu, Y.H., Wieckowska, A., Dembic, M., Bruun, G.H., Krainer,
652   A.R. and Andresen, B.S. (2017). RNA-sequencing of a mouse-model of spinal muscular atrophy reveals
653   tissue-wide changes in splicing of U12-dependent introns. *Nucleic Acids Research*. 45(1), 395-416.

654   Doyle, M. and Kiebler, M.A. (2011). Mechanisms of dendritic mRNA transport and its role in synaptic
655   tagging. *The EMBO Journal*. 30(17), 3540-3552.

656   Fallini, C., Donlin-Asp, P.G., Rouanet, J.P., Bassell, G.J. and Rossoll, W. (2016). Deficiency of the Survival of
657   Motor Neuron Protein Impairs mRNA Localization and Local Translation in the Growth Cone of Motor
658   Neurons. *The Journal of Neuroscience*. 36(13), 3811-3820.

659   Fallini, C., Rouanet, J.P., Donlin-Asp, P.G., Guo, P., Zhang, H., Singer, R.H., Rossoll, W. and Bassell, G.J.
660   (2014). Dynamics of survival of motor neuron (SMN) protein interaction with the mRNA-binding protein
661   IMP1 facilitates its trafficking into motor neuron axons. *Developmental Neurobiology*. 74(3), 319-332.

662   Fallini, C., Zhang, H., Su, Y., Silani, V., Singer, R.H., Rossoll, W. and Bassell, G.J. (2011). The Survival of Motor
663   Neuron (SMN) Protein Interacts with the mRNA-Binding Protein HuD and Regulates Localization of Poly(A)
664   mRNA in Primary Motor Neuron Axons. *The Journal of Neuroscience*. 31(10), 3914-3925.

665   Finkel, R.S., Chiriboga, C.A., Vajsar, J., Day, J.W., Montes, J., De Vivo, D.,C., Yamashita, M., Rigo, F., Hung, G.,
666   Schneider, E., Norris, D.A., Xia, S., Bennett, C.F. and Bishop, K.M. (2016). Treatment of infantile-onset spinal
667   muscular atrophy with nusinersen: a phase 2, open-label, dose-escalation study. *The Lancet*. 388(10063),
668   3017-3026.

669   Fischer, U., Englbrecht, C. and Chari, A. (2011). Biogenesis of spliceosomal small nuclear ribonucleoproteins.
670   *Wiley Interdisciplinary Reviews: RNA*. 2(5), 718-731.

671   Fischer, U., Liu, Q. and Dreyfuss, G. (1997). The SMN–SIP1 Complex Has an Essential Role in Spliceosomal
672   snRNP Biogenesis. *Cell*. 90(6), 1023-1029.

673   Francke, F., Ward, R.J., Jenkins, L., Kellett, E., Richter, D., Milligan, G. and Bächner, D. (2006). Interaction of
674   Neurochondrin with the Melanin-concentrating Hormone Receptor 1 Interferes with G Protein-coupled
675   Signal Transduction but Not Agonist-mediated Internalization. *Journal of Biological Chemistry*. 281(43),
676   32496-32507.

677   Gabanella, F., Butchbach, M.E.R., Saieva, L., Carissimi, C., Burghes, A.H.M. and Pellizzoni, L. (2007).
678   Ribonucleoprotein Assembly Defects Correlate with Spinal Muscular Atrophy Severity and Preferentially
679   Affect a Subset of Spliceosomal snRNPs. *Plos One*. 2(9), e921.

680   Gonsalvez, G.B., Rajendra, T.K., Wen, Y., Praveen, K. and Matera, A.G. (2010). Sm proteins specify germ cell
681   fate by facilitating *oskar* mRNA localization. *Development*. 137(14), 2341-2351.

682   Guo, X., Farías, G.G., Mattera, R. and Bonifacino, J.S. (2016). Rab5 and its effector FHF contribute to
683   neuronal polarity through dynein-dependent retrieval of somatodendritic proteins from the axon.
684   *Proceedings of the National Academy of Sciences*. 113(36), E5318-E5327.

685   Harms, M.B., Allred, P., Gardner, R., Fernandes Filho, J.A., Florence, J., Pestronk, A., Al-Lozi, M. and Baloh,
686   R.H. (2010). Dominant spinal muscular atrophy with lower extremity predominance: Linkage to 14q32.
687   *Neurology*. 75(6), 539-546.

688   Harms, M.B., Ori-McKenney, K.M., Scoto, M., Tuck, E.P., Bell, S., Ma, D., Masi, S., Allred, P., Al-Lozi, M.,
689   Reilly, M.M., Miller, L.J., Jani-Acsadi, A., Pestronk, A., Shy, M.E., Muntoni, F., Vallee, R.B. and Baloh, R.H.
690   (2012). Mutations in the tail domain of DYNC1H1 cause dominant spinal muscular atrophy. *Neurology*.
691   78(22), 1714-1720.

692   Hausmann, S., Zheng, S., Costanzo, M., Brost, R.L., Garcin, D., Boone, C., Shuman, S. and Schwer, B. (2008).
693   Genetic and Biochemical Analysis of Yeast and Human Cap Trimethylguanosine Synthase: FUNCTIONAL
694   OVERLAP OF 2,2,7-TRIMETHYLGUANOSINE CAPS, SMALL NUCLEAR RIBONUCLEOPROTEIN COMPONENTS,
695   PRE-mRNA SPLICING FACTORS, AND RNA DECAY PATHWAYS. *Journal of Biological Chemistry*. 283(46),
696   31706-31718.

697   Holt, C. and Schuman, E. (2013). The Central Dogma Decentralized: New Perspectives on RNA Function and
698   Local Translation in Neurons. *Neuron*. 80(3), 648-657.

699   Hosseinibarkooie, S., Peters, M., Torres-Benito, L., Rastetter, R., Hupperich, K., Hoffmann, A., Mendoza-
700   Ferreira, N., Kaczmarek, A., Janzen, E., Milbradt, J., Lamkemeyer, T., Rigo, F., Bennett, C. ., Guschlbauer, C.,
701   Büschges, A., Hammerschmidt, M., Riessland, M., Kye, M., Clemen, C. and Wirth, B. (2016). The Power of
702   Human Protective Modifiers: PLS3 and CORO1C Unravel Impaired Endocytosis in Spinal Muscular Atrophy
703   and Rescue SMA Phenotype. *The American Journal of Human Genetics*. 99(3), 647-665.

704   Hsieh-Li, H., Chang, J., Jong, Y., Wu, M., Wang, N.M., Tsai, C.H. and Li, H. (2000). A mouse model for spinal
705   muscular atrophy. *Nature Genetics*. 24(1), 66-70.

706   Huber, K.M., Kayser, M.S. and Bear, M.F. (2000). Role for Rapid Dendritic Protein Synthesis in Hippocampal
707   mGluR-Dependent Long-Term Depression. *Science*. 288(5469), 1254-1256.

708   Huntriss, J.D., Latchman, D.S. and Williams, D.G. (1993). The snRNP core protein SmB and tissue-specific
709   SmN protein are differentially distributed between snRNP particles. *Nucleic Acids Research*. 21(17), 4047-
710   4053.

711   Huo, Q., Kayikci, M., Odermatt, P., Meyer, K., Michels, O., Saxena, S., Ule, J. and Schuemperli, D. (2014).
712   Splicing changes in SMA mouse motoneurons and SMN-depleted neuroblastoma cells: Evidence for
713   involvement of splicing regulatory proteins. *RNA Biology*. 11(11), 1430-1446.

714 Jeronimo, C., Forget, D., Bouchard, A., Li, Q., Chua, G., Poitras, C., Thérien, C., Bergeron, D., Bourassa, S.,
715 Greenblatt, J., Chabot, B., Poirier, G.G., Hughes, T.R., Blanchette, M., Price, D.H. and Coulombe, B. (2007).
716 Systematic Analysis of the Protein Interaction Network for the Human Transcription Machinery Reveals the
717 Identity of the 7SK Capping Enzyme. *Molecular Cell*. 27(2), 262-274.

718 Kang, H. and Schuman, E.M. (1996). A Requirement for Local Protein Synthesis in Neurotrophin-Induced
719 Hippocampal Synaptic Plasticity. *Science*. 273(5280), 1402-1406.

720 Keller, A., Nesvizhskii, A.I., Kolker, E. and Aebersold, R. (2002). Empirical Statistical Model To Estimate the
721 Accuracy of Peptide Identifications Made by MS/MS and Database Search. *Analytical Chemistry*. 74(20),
722 5383-5392.

723 Kofler, M., Heuer, K., Zech, T. and Freund, C. (2004). Recognition Sequences for the GYF Domain Reveal a
724 Possible Spliceosomal Function of CD2BP2. *Journal of Biological Chemistry*. 279(27), 28292-28297.

725 Kofler, M., Motzny, K. and Freund, C. (2005). GYF Domain Proteomics Reveals Interaction Sites in Known
726 and Novel Target Proteins. *Molecular & Cellular Proteomics*. 4(11), 1797-1811

727 Lee, M., Lin, Y., Deng, Y., Hsu, W., Shen, C., Cheng, Y., Huang, Y. and Li, C. (2014). Modulation of alternative
728 splicing by expression of small nuclear ribonucleoprotein polypeptide N. *FEBS Journal*. 281(23), 5194-5207.

729 Lefebvre, S., Burlet, P., Liu, Q., Bertrandy, S., Clermont, O., Munnich, A., Dreyfuss, G. and Melki, J. (1997).
730 Correlation between severity and SMN protein level in spinal muscular atrophy. *Nature Genetics*. 16(3),
731 265-269.

732 Lefebvre, S., Bürglen, L., Reboullet, S., Clermont, O., Burlet, P., Viollet, L., Benichou, B., Cruaud, C.,
733 Millasseau, P., Zeviani, M., Le Paslier, D., Frézal, J., Cohen, D., Weissenbach, J., Munnich, A. and Melki, J.
734 (1995). Identification and characterization of a spinal muscular atrophy-determining gene. *Cell*. 80(1), 155-
735 165.

736 Li, D.K., Tisdale, S., Lotti, F. and Pellizzoni, L. (2014). SMN control of RNP assembly: From post-
737 transcriptional gene regulation to motor neuron disease. *Seminars in Cell & Developmental Biology*. 32, 22-
738 29.

739 Li, H., Custer, S.K., Gilson, T., Hao, L.T., Beattie, C.E. and Androphy, E.J. (2015). α-COP binding to the survival
740 motor neuron protein SMN is required for neuronal process outgrowth. *Human Molecular Genetics*. 24(25),
741 7295-7307.

742 Liu, Q. and Dreyfuss, G. (1996). A novel nuclear structure containing the survival of motor neurons protein.
743 *The EMBO Journal*. 15(14), 3555-3565.

744 Liu, Q., Fischer, U., Wang, F. and Dreyfuss, G. (1997). The Spinal Muscular Atrophy Disease Gene Product,
745 SMN, and Its Associated Protein SIP1 Are in a Complex with Spliceosomal snRNP Proteins. *Cell*. 90(6), 1013-
746 1021.

747 Lodish, H., Berk, A., Zipursky, L., Matsudaira, P., Baltimore, D. and Darnell, J. (2000). Section 5.2: Purification
748 of Cells and their parts. *Molecular Cell Biology*. 4th ed. New York: W H Freeman.

749 Lorson, C.L. and Androphy, E.J. (2000). An exonic enhancer is required for inclusion of an essential exon in
750 the SMA-determining gene SMN. *Human Molecular Genetics*. 9(2), 259-265.

751 Lorson, C.L., Hahnen, E., Androphy, E.J. and Wirth, B. (1999). A single nucleotide in the SMN gene regulates
752 splicing and is responsible for spinal muscular atrophy. *Proceedings of the National Academy of Sciences*.
753 96(11), 6307-6311.

754 Lotti, F., Imlach, W., Saieva, L., Beck, E., Hao, L., Li, D., Jiao, W., Mentis, G., Beattie, C., McCabe, B. and
755 Pellizzoni, L. (2012). An SMN-Dependent U12 Splicing Event Essential for Motor Circuit Function. *Cell*.
756 151(2), 440-454.

757 Martinez-Carrera, L. and Wirth, B. (2015). Dominant spinal muscular atrophy is caused by mutations in
758 BICD2, an important golgin protein. *Frontiers in Neuroscience*. 9, 401.

759 Matosin, N., Fernandez-Enright, F., Fung, S.J., Lum, J.S., Engel, M., Andrews, J.L., Huang, X., Weickert, C.S.
760 and Newell, K.A. (2015). Alterations of mGluR5 and its endogenous regulators Norbin, Tamalin and Preso1
761 in schizophrenia: towards a model of mGluR5 dysregulation. *Acta Neuropathologica*. 130(1), 119-129.

762 Meister, G., Buhler, D., Pillai, R., Lottspeich, F. and Fischer, U. (2001). A multiprotein complex mediates the
763 ATP-dependent assembly of spliceosomal U snRNPs. *Nature Cell Biology*. 3(11), 945-949.

764 Meister, G. and Fischer, U. (2002). Assisted RNP assembly: SMN and PRMT5 complexes cooperate in the
765 formation of spliceosomal UsnRNPs. *The EMBO Journal*. 21(21), 5853-5863.

766 Mohr, H. and Völkl, A. (2001). Ultracentrifugation. *eLS*John Wiley & Sons, Ltd.

767 Monani, U.R. (2005). Spinal Muscular Atrophy: A Deficiency in a Ubiquitous Protein; a Motor Neuron-
768 Specific Disease. *Neuron*. 48(6), 885-895.

769 Monani, U.R., Lorson, C.L., Parsons, D.W., Prior, T.W., Androphy, E.J., Burghes, A.H.M. and McPherson, J.D.
770 (1999). A Single Nucleotide Difference That Alters Splicing Patterns Distinguishes the SMA Gene SMN1
771 From the Copy Gene SMN2. *Human Molecular Genetics*. 8(7), 1177-1183.

772 Monani, U.R., Sendtner, M., Coovert, D.D., Parsons, D.W., Andreassi, C., Le, T.T., Jablonka, S., Schrank, B.,
773 Rossol, W., Prior, T.W., Morris, G.E. and Burghes, A.H.M. (2000). The human centromeric survival motor
774 neuron gene (SMN2) rescues embryonic lethality in Smn–/– mice and results in a mouse with spinal
775 muscular atrophy. *Human Molecular Genetics*. 9(3), 333-339.

776 Mourão, A., Bonnal, S., Soni, K., Warner, L., Bordonné, R., Valcárcel, J. and Sattler, M. (2016). Structural
777 basis for the recognition of spliceosomal SmN/B/B' proteins by the RBM5 OCRE domain in splicing
778 regulation. *eLife*. 5, e14707.

779 Nesvizhskii, A.I., Keller, A., Kolker, E. and Aebersold, R. (2003). A Statistical Model for Identifying Proteins by
780 Tandem Mass Spectrometry. *Analytical Chemistry*. 75(17), 4646-4658.

781 Neveling, K., Martinez-Carrera, L., Hölker, I., Heister, A., Verrips, A., Hosseini-Barkooie, S., Gilissen, C.,
782 Vermeer, S., Pennings, M., Meijer, R., te Riele, M., Frijns, C.M., Suchowersky, O., MacLaren, L., Rudnik-
783 Schöneborn, S., Sinke, R., Zerres, K., Lowry, R. ., Lemmink, H., Garbes, L., Veltman, J., Schelhaas, H.,
784 Scheffer, H. and Wirth, B. (2013). Mutations in *BICD2*, which Encodes a Golgin and Important Motor
785 Adaptor, Cause Congenital Autosomal-Dominant Spinal Muscular Atrophy. *The American Journal of Human*
786 *Genetics*. 92(6), 946-954.

787 Niu, Q., Wang, X., Shi, M. and Jin, Q. (2015). A novel DYNC1H1 mutation causing spinal muscular atrophy
788 with lower extremity predominance. *Neurology Genetics*. 1(2).

789 Oates, E., Rossor, A., Hafezparast, M., Gonzalez, M., Speziani, F., MacArthur, D., Lek, M., Cottenie, E., Scoto,
790 M., Foley, A. ., Hurles, M., Houlden, H., Greensmith, L., Auer-Grumbach, M., Pieber, T., Strom, T., Schule, R.,
791 Herrmann, D., Sowden, J., Acsadi, G., Menezes, M., Clarke, N., Züchner, S., Muntoni, F., North, K. and Reilly,
792 M. (2013). Mutations in *BICD2* Cause Dominant Congenital Spinal Muscular Atrophy and Hereditary Spastic
793 Paraplegia. *The American Journal of Human Genetics*. 92(6), 965-973.

794 Ohoka, Y., Hirotani, M., Sugimoto, H., Fujioka, S., Furuyama, T. and Inagaki, S. (2001). Semaphorin 4C, a
795 transmembrane semaphorin,associates with a Neurite-Outgrowth-Related Protein, SFAP75. *Biochemical*
796 *and Biophysical Research Communications*. 280(1), 237-243.

797 Oku, S., Takahashi, N., Fukata, Y. and Fukata, M. (2013). In Silico Screening for Palmitoyl Substrates Reveals
798 a Role for DHHC1/3/10 (zDHHC1/3/11)-mediated Neurochondrin Palmitoylation in Its Targeting to Rab5-
799 positive Endosomes. *Journal of Biological Chemistry*. 288(27), 19816-19829.

800 Oprea, G.E., Kröber, S., McWhorter, M.L., Rossoll, W., Müller, S., Krawczak, M., Bassell, G.J., Beattie, C.E.
801 and Wirth, B. (2008). Plastin 3 Is a Protective Modifier of Autosomal Recessive Spinal Muscular Atrophy.
802 *Science*. 320(5875), 524-527.

803 Ozcelik, T., Leff, S., Robinson, W., Donlon, T., Lalande, M., Sanjines, E., Schinzel, A. and Francke, U. (1992).
804 Small nuclear ribonucleoprotein polypeptide N (SNRPN), an expressed gene in the Prader-Willi syndrome
805 critical region. *Nature Genetics*. 2(4), 265-269.

806 Pan, D., Barber, M.A., Hornigold, K., Baker, M.J., Toth, J.M., Oxley, D. and Welch, H.C.E. (2016). Norbin
807 Stimulates the Catalytic Activity and Plasma Membrane Localization of the Guanine-Nucleotide Exchange
808 Factor P-Rex1. *Journal of Biological Chemistry*. 291(12), 6359-6375.

809 Passini, M.A., Bu, J., Richards, A.M., Kinnecom, C., Sardi, S.P., Stanek, L.M., Hua, Y., Rigo, F., Matson, J.,
810 Hung, G., Kaye, E.M., Shihabuddin, L.S., Krainer, A.R., Bennett, C.F. and Cheng, S.H. (2011). Antisense
811 Oligonucleotides Delivered to the Mouse CNS Ameliorate Symptoms of Severe Spinal Muscular Atrophy.
812 *Science Translational Medicine*. 3(72), 72ra18-72ra18.

813 Peeters, K., Bervoets, S., Chamova, T., Litvinenko, I., De Vriendt, E., Bichev, S., Kancheva, D., Mitev, V.,
814 Kennerson, M., Timmerman, V., De Jonghe, P., Tournev, I., MacMillan, J. and Jordanova, A. (2015). Novel
815 Mutations in the DYNC1H1 Tail Domain Refine the Genetic and Clinical Spectrum of Dyneinopathies.
816 *Human Mutation*. 36(3), 287-291.

817 Peeters, K., Litvinenko, I., Asselbergh, B., Almeida-Souza, L., Chamova, T., Geuens, T., Ydens, E., Zimoń, M.,
818 Irobi, J., De Vriendt, E., De Winter, V., Ooms, T., Timmerman, V., Tournev, I. and Jordanova, A. (2013).
819 Molecular Defects in the Motor Adaptor BICD2 Cause Proximal Spinal Muscular Atrophy with Autosomal-
820 Dominant Inheritance. *The American Journal of Human Genetics*. 92(6), 955-964.

821 Pellizzoni, L., Yong, J. and Dreyfuss, G. (2002). Essential Role for the SMN Complex in the Specificity of
822 snRNP Assembly. *Science*. 298(5599), 1775-1779.

823 Peter, C.J., Evans, M., Thayanithy, V., Taniguchi-Ishigaki, N., Bach, I., Kolpak, A., Bassell, G.J., Rossoll, W.,
824 Lorson, C.L., Bao, Z. and Androphy, E.J. (2011). The COPI vesicle complex binds and moves with survival
825 motor neuron within axons. *Human Molecular Genetics*. 20(9), 1701-1711.

826 Prescott, A.R., Bales, A., James, J., Trinkle-Mulcahy, L. and Sleeman, J.E. (2014). Time-resolved quantitative
827 proteomics implicates the core snRNP protein SmB together with SMN in neural trafficking. *Journal of Cell*
828 *Science*. 127(4), 812-827.

829 Prior, T.W., Swoboda, K.J., Scott, H.D. and Hejmanowski, A.Q. (2004). Homozygous SMN1 deletions in
830 unaffected family members and modification of the phenotype by SMN2. *American Journal of Medical*
831 *Genetics Part A*. 130A(3), 307-310.

832 Punetha, J., Monges, S., Franchi, M.E., Hoffman, E.P., Cirak, S. and Tesi-Rocha, C. (2015). Exome Sequencing
833 Identifies DYNC1H1 Variant Associated With Vertebral Abnormality and Spinal Muscular Atrophy With
834 Lower Extremity Predominance. *Pediatric Neurology*. 52(2), 239-244.

835 Riessland, M., Kaczmarek, A., Schneider, S., Swoboda, K.J., Löhr, H., Bradler, C., Grysko, V., Dimitriadi, M.,
836 Hosseinibarkooie, S., Torres-Benito, L., Peters, M., Upadhyay, A., Biglari, N., Kröber, S., Hölker, I., Garbes, L.,
837 Gilissen, C., Hoischen, A., Nürnberg, G., Nürnberg, P., Walter, M., Rigo, F., Bennett, C.F., Kye, M.J., Hart,
838 A.C., Hammerschmidt, M., Kloppenburg, P. and Wirth, B. (2017). Neurocalcin Delta Suppression Protects
839 against Spinal Muscular Atrophy in Humans and across Species by Restoring Impaired Endocytosis. *The*
840 *American Journal of Human Genetics*. 100(2), 297-315.

841 Renvoisé, B., Khoobarry, K., Gendron, M., Cibert, C., Viollet, L. and Lefebvre, S. (2006). Distinct domains of
842 the spinal muscular atrophy protein SMN are required for targeting to Cajal bodies in mammalian cells.
843 *Journal of Cell Science*. 119(4), 680.

844 Rossoll, W., Jablonka, S., Andreassi, C., Kröning, A., Karle, K., Monani, U.R. and Sendtner, M. (2003a). Smn,
845 the spinal muscular atrophy–determining gene product, modulates axon growth and localization of ß-actin
846 mRNA in growth cones of motoneurons. *The Journal of Cell Biology*. 163(4), 801-812.

847 Rossoll, W., Jablonka, S., Andreassi, C., Kröning, A., Karle, K., Monani, U.R. and Sendtner, M. (2003b). Smn,
848 the spinal muscular atrophy–determining gene product, modulates axon growth and localization of ß-actin
849 mRNA in growth cones of motoneurons. *The Journal of Cell Biology*. 163(4), 801-812.

850 Rossoll, W., Kröning, A., Ohndorf, U., Steegborn, C., Jablonka, S. and Sendtner, M. (2002). Specific
851 interaction of Smn, the spinal muscular atrophy determining gene product, with hnRNP-R and gry-
852 rbp/hnRNP-Q: a role for Smn in RNA processing in motor axons?. *Human Molecular Genetics*. 11(1), 93-105.

853 Rossor, A.M., Oates, E.C., Salter, H.K., Liu, Y., Murphy, S.M., Schule, R., Gonzalez, M.A., Scoto, M., Phadke,
854 R., Sewry, C.A., Houlden, H., Jordanova, A., Tournev, I., Chamova, T., Litvinenko, I., Zuchner, S., Herrmann,
855 D.N., Blake, J., Sowden, J.E., Acsadi, G., Rodriguez, M.L., Menezes, M.P., Clarke, N.F., Auer Grumbach, M.,
856 Bullock, S.L., Muntoni, F., Reilly, M.M. and North, K.N. (2015). Phenotypic and molecular insights into spinal
857 muscular atrophy due to mutations in BICD2. *Brain*. 138(2), 293-310.

858 Satoh, D., Sato, D., Tsuyama, T., Saito, M., Ohkura, H., Rolls, M.M., Ishikawa, F. and Uemura, T. (2008).
859 Spatial control of branching within dendritic arbors by dynein-dependent transport of Rab5-endosomes.
860 *Nature Cell Biology*. 10(10), 1164-1171.

861 Schmauss, C., Brines, M.L. and Lerner, M.R. (1992). The gene encoding the small nuclear ribonucleoprotein-
862 associated protein N is expressed at high levels in neurons. *Journal of Biological Chemistry*. 267(12), 8521-
863 8529.

864 Schrank, B., Götz, R., Gunnersen, J.M., Ure, J.M., Toyka, K.V., Smith, A.G. and Sendtner, M. (1997).
865 Inactivation of the survival motor neuron gene, a candidate gene for human spinal muscular atrophy, leads
866 to massive cell death in early mouse embryos. *Proceedings of the National Academy of Sciences*. 94(18),
867 9920-9925.

868 Scoto, M., Rossor, A.M., Harms, M.B., Cirak, S., Calissano, M., Robb, S., Manzur, A.Y., Martínez Arroyo, A.,
869 Rodriguez Sanz, A., Mansour, S., Fallon, P., Hadjikoumi, I., Klein, A., Yang, M., De Visser, M., Overweg-
870 Plandsoen, W.C.G.(., Baas, F., Taylor, J.P., Benatar, M., Connolly, A.M., Al-Lozi, M.T., Nixon, J., de Goede,

C.G.E.L., Foley, A.R., Mcwilliam, C., Pitt, M., Sewry, C., Phadke, R., Hafezparast, M., Chong, W.K.", Mercuri, E., Baloh, R.H., Reilly, M.M. and Muntoni, F. (2015). Novel mutations expand the clinical spectrum of DYNC1H1-associated spinal muscular atrophy. *Neurology*. 84(7), 668-679.

Shevchenko, A., Wilm, M., Vorm, O. and Mann, M. (1996). Mass Spectrometric Sequencing of Proteins from Silver-Stained Polyacrylamide Gels. *Analytical Chemistry*. 68(5), 850-858.

Shinozaki, K., Kume, H., Kuzume, H., Obata, K. and Maruyama, K. (1999). Norbin, a neurite-outgrowth-related protein, is a cytosolic protein localized in the somatodendritic region of neurons and distributed prominently in dendritic outgrowth in Purkinje cells1. *Molecular Brain Research*. 71(2), 364-368.

Shinozaki, K., Maruyama, K., Kume, H., Kuzume, H. and Obata, K. (1997). A Novel Brain Gene, Norbin, Induced by Treatment of Tetraethylammonium in Rat Hippocampal Slice and Accompanied with Neurite-Outgrowth in Neuro 2a Cells. *Biochemical and Biophysical Research Communications*. 240(3), 766-771.

Shpargel, K.B. and Matera, A.G. (2005). Gemin proteins are required for efficient assembly of Sm-class ribonucleoproteins. *Proceedings of the National Academy of Sciences of the United States of America*. 102(48), 17372-17377.

Sleeman, J. and Lamond, A. (1999). Newly assembled snRNPs associate with coiled bodies before speckles, suggesting a nuclear snRNP maturation pathway. *Current Biology*. 9(19), 1065-1074.

Sleeman, J. (2013). Small nuclear RNAs and mRNAs: linking RNA processing and transport to spinal muscular atrophy. *Biochemical Society Transactions*. 41, 871-875.

Sleeman, J.E., Ajuh, P. and Lamond, A.I. (2001). snRNP protein expression enhances the formation of Cajal bodies containing p80-coilin and SMN. *Journal of Cell Science*. 114(24), 4407-4419.

Sleeman, J.E., Trinkle-Mulcahy, L., Prescott, A.R., Ogg, S.C. and Lamond, A.I. (2003). Cajal body proteins SMN and Coilin show differential dynamic behaviour in vivo. *Journal of Cell Science*. 116(10), 2039-2050.

Sleigh, J.N., Gillingwater, T.H. and Talbot, K. (2011). The contribution of mouse models to understanding the pathogenesis of spinal muscular atrophy. *Disease Models & Mechanisms*. 4(4), 457-467.

Stark, H., Dube, P., Luhrmann, R. and Kastner, B. (2001). Arrangement of RNA and proteins in the spliceosomal U1 small nuclear ribonucleoprotein particle. *Nature*. 409(6819), 542.

Strickland, A.V., Schabhüttl, M., Offenbacher, H., Synofzik, M., Hauser, N.S., Brunner-Krainz, M., Gruber-Sedlmayr, U., Moore, S.A., Windhager, R., Bender, B., Harms, M., Klebe, S., Young, P., Kennerson, M., Garcia, A.S.M., Gonzalez, M.A., Züchner, S., Schule, R., Shy, M.E. and Auer-Grumbach, M. (2015). Mutation screen reveals novel variants and expands the phenotypes associated with DYNC1H1. *Journal of Neurology*. 262(9), 2124-2134.

Synofzik, M., Martinez-Carrera, L., Lindig, T., Schöls, L. and Wirth, B. (2014). Dominant spinal muscular atrophy due to *BICD2*: a novel mutation refines the phenotype. *J Neurol Neurosurg Psychiatry*. 85(5), 590.

Ting, C., Wen, H., Liu, H., Hsieh-Li, H., Li, H. and Lin-Chao, S. (2012). The Spinal Muscular Atrophy Disease Protein SMN Is Linked to the Golgi Network. *Plos One*. 7(12), e51826.

Tisdale, S. and Pellizzoni, L. (2015). Disease Mechanisms and Therapeutic Approaches in Spinal Muscular Atrophy. *The Journal of Neuroscience*. 35(23), 8691-8700.

908 Todd, A.G., Morse, R., Shaw, D.J., McGinley, S., Stebbings, H. and Young, P.J. (2010a). SMN, Gemin2 and
909 Gemin3 Associate with β-Actin mRNA in the Cytoplasm of Neuronal Cells In Vitro. *Journal of Molecular*
910 *Biology*. 401(5), 681-689.

911 Todd, A.G., Morse, R., Shaw, D.J., Stebbings, H. and Young, P.J. (2010b). Analysis of SMN-neurite granules:
912 Core Cajal body components are absent from SMN-cytoplasmic complexes. *Biochemical and Biophysical*
913 *Research Communications*. 397(3), 479-485.

914 Trinkle-Mulcahy, L., Boulon, S., Lam, Y.W., Urcia, R., Boisvert, F., Vandermoere, F., Morrice, N.A., Swift, S.,
915 Rothbauer, U., Leonhardt, H. and Lamond, A. (2008). Identifying specific protein interaction partners using
916 quantitative mass spectrometry and bead proteomes. *The Journal of Cell Biology*. 183(2), 223-239.

917 Tsurusaki, Y., Saitoh, S., Tomizawa, K., Sudo, A., Asahina, N., Shiraishi, H., Ito, J., Tanaka, H., Doi, H., Saitsu,
918 H., Miyake, N. and Matsumoto, N. (2012). A DYNC1H1 mutation causes a dominant spinal muscular atrophy
919 with lower extremity predominance. *Neurogenetics*. 13(4), 327-332.

920 Urlaub, H., Raker, V., Kostka, S. and Luhrmann, R. (2001). Sm protein-Sm site RNA interactions within the
921 inner ring of the spliceosomal snRNP core structure. *Embo Journal*. 20(1-2), 187-196.

922 Vonderheit, A. and Helenius, A. (2005). Rab7 Associates with Early Endosomes to Mediate Sorting and
923 Transport of Semliki Forest Virus to Late Endosomes. *PLOS Biology*. 3(7), e233.

924 Wan, L., Battle, D.J., Yong, J., Gubitz, A.K., Kolb, S.J., Wang, J. and Dreyfuss, G. (2005). The Survival of Motor
925 Neurons Protein Determines the Capacity for snRNP Assembly: Biochemical Deficiency in Spinal Muscular
926 Atrophy. *Molecular and Cellular Biology*. 25(13), 5543-5551.

927 Wang, H., Duan, X., Ren, Y., Liu, Y., Huang, M., Liu, P., Wang, R., Gao, G., Zhou, L., Feng, Z. and Zheng, W.
928 (2013). FoxO3a Negatively Regulates Nerve Growth Factor-Induced Neuronal Differentiation Through
929 Inhibiting the Expression of Neurochondrin in PC12 Cells. *Molecular Neurobiology*. 47(1), 24-36.

930 Wang, H., Westin, L., Nong, Y., Birnbaum, S., Bendor, J., Brismar, H., Nestler, E., Aperia, A., Flajolet, M. and
931 Greengard, P. (2009). Norbin Is an Endogenous Regulator of Metabotropic Glutamate Receptor 5 Signaling.
932 *Science*. 326(5959), 1554-1557.

933 Ward, R.J., Jenkins, L. and Milligan, G. (2009). Selectivity and functional consequences of interactions of
934 family A G protein-coupled receptors with neurochondrin and periplakin. *Journal of Neurochemistry*.
935 109(1), 182-192.

936 Winkler, C., Eggert, C., Gradl, D., Meister, G., Giegerich, M., Wedlich, D., Laggerbauer, B. and Fischer, U.
937 (2005). Reduced U snRNP assembly causes motor axon degeneration in an animal model for spinal
938 muscular atrophy. *Genes & Development*. 19(19), 2320-2330.

939 Xiong, X., Vogler, G., Kurthkoti, K., Samsonova, A. and Zhou, R. (2015). SmD1 Modulates the miRNA
940 Pathway Independently of Its Pre-mRNA Splicing Function. *PLOS Genetics*. 11(8), e1005475.

941 Zhang, H.L., Pan, F., Hong, D., Shenoy, S.M., Singer, R.H. and Bassell, G.J. (2003). Active Transport of the
942 Survival Motor Neuron Protein and the Role of Exon-7 in Cytoplasmic Localization. *The Journal of*
943 *Neuroscience*. 23(16), 6627-6637.

944 Zhang, H., Xing, L., Rossoll, W., Wichterle, H., Singer, R.H. and Bassell, G.J. (2006a). Multiprotein Complexes
945 of the Survival of Motor Neuron Protein SMN with Gemins Traffic to Neuronal Processes and Growth Cones
946 of Motor Neurons. *The Journal of Neuroscience*. 26(33), 8622-8632.

947   Zhang, Z., Lotti, F., Dittmar, K., Younis, I., Wan, L., Kasim, M. and Dreyfuss, G. (2008). SMN Deficiency
948   Causes Tissue-Specific Perturbations in the Repertoire of snRNAs and Widespread Defects in Splicing. *Cell*.
949   133(4), 585-600.

950

951
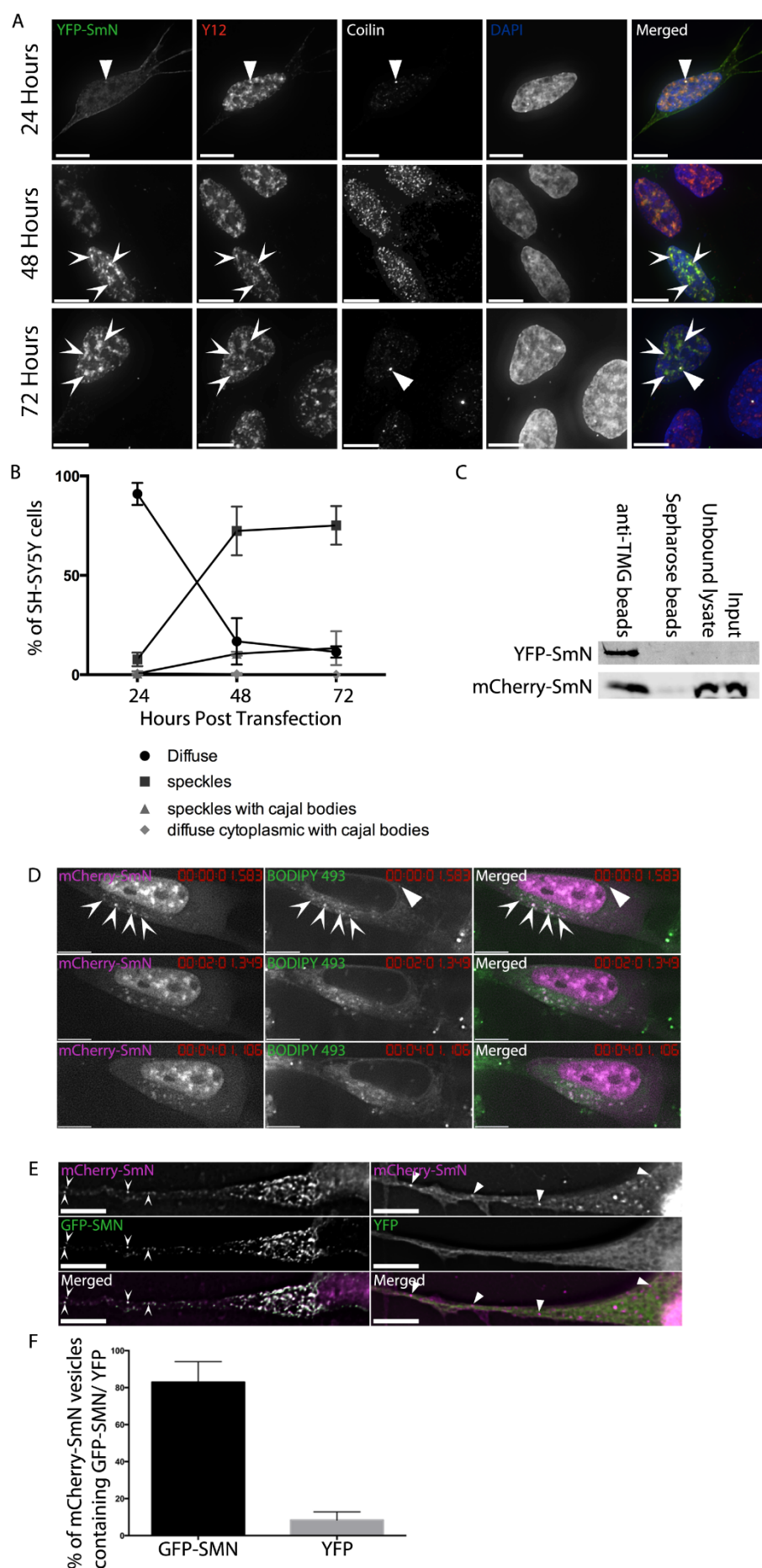
952   *Figure 1: SmN exhibits similar behaviour to SmB in SH-SY5Y cells.* *A) SH-SY5Y cells transiently expressing*
953   *YFP-SmN and fixed after 24, 48 and 72 hours show variations in distribution of the YFP-SmN with time.*
954   *Immunostaining with Y12 (red on overlay) and anti-coilin (white on overlay) shows splicing speckles*
955   *(arrowheads) and Cajal Bodies (CBs, triangles) respectively. Images are deconvolved z-stacks with 0.2 μm*
956   *spacing. Bar=7μm. B) SmN initially localises diffusely in the cytoplasm, before localising to speckles at the 48*
957   *and 72 hour time-points. 3 independent experiments, n=100 cells per experiment. Data shown is mean +/-*
958   *SD). C) Western blot analysis of snRNPs immunprecipiated using TMG beads (left hand lane) confirms that*
959   *both YFP-SmN (detected with anti-YFP, top row) and mCherry-SmN (detected with anti-mCherry, bottom*
960   *row) are incorporated into snRNPs. D) mCherry-SmN cytoplasmic structures are mobile and stain with the*
961   *lipophilic dye BODIPY 493. Arrows identify mCherry-SmN structures stained with BODIPY 493, triangles*
962   *identify BODIPY 493-stained vesicles not containing mCherry-SmN. Cells were imaged approximately every 4*
963   *seconds for 9 minutes. Images are single deconvolved z-sections. Bar=7μm. E) mCherry-SmN and GFP-SMN*
964   *co-localise in cytoplasmic foci in SH-SY5Y cells (arrowheads in left hand panels), whereas YFP alone shows*
965   *no accumulation in mCherry-SmN foci (triangles in right hand panels). White signal on the overlay indicates*
966   *areas of co-localisation. Images are single deconvolved z-sections. Bar=7μm. F) Comparison of the*
967   *percentage of mCherry-SmN vesicles per cell co-localising with GFP-SMN to those showing co-incidental*
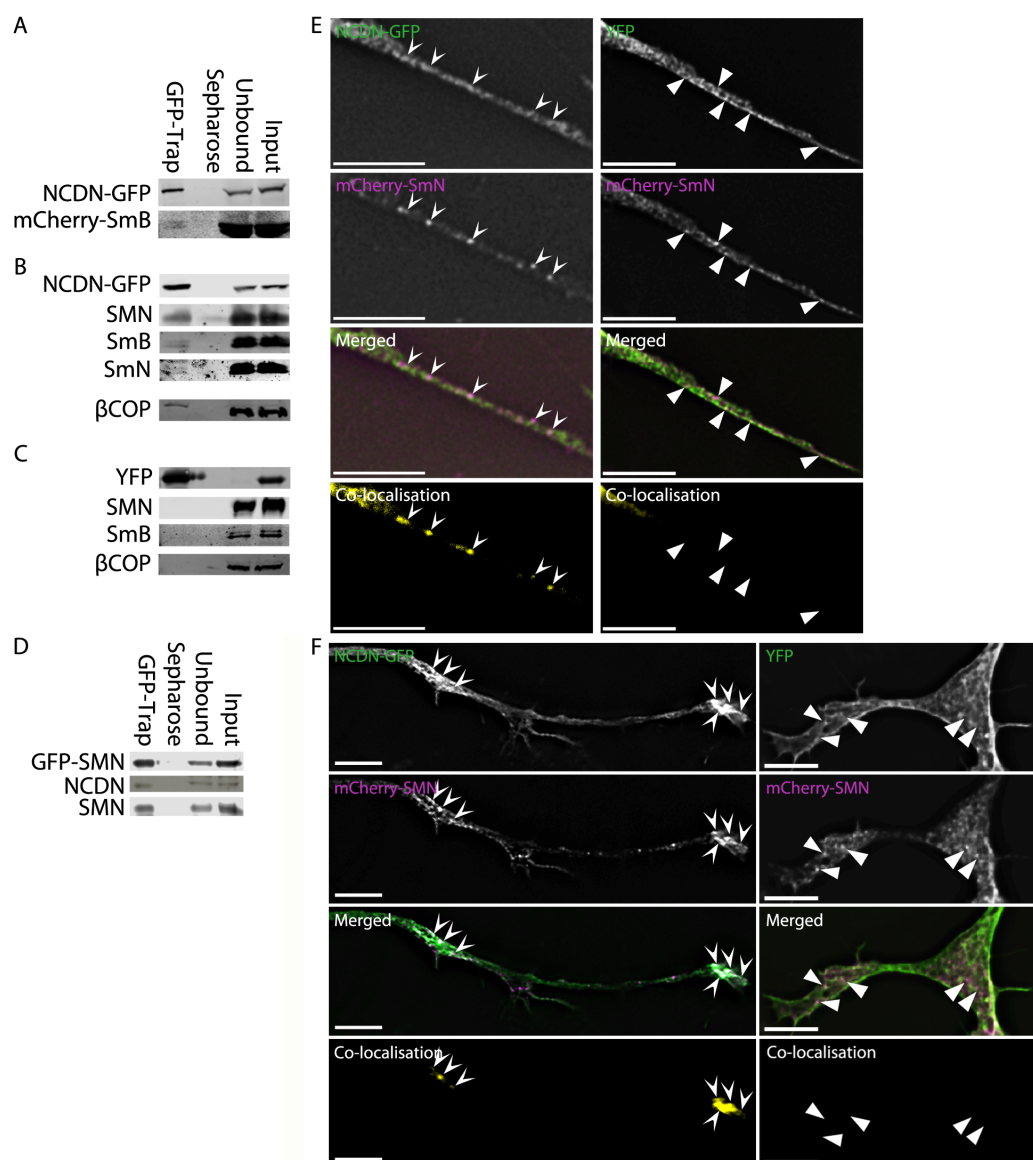968   *overlap with YFP alone confirms the co-localisation (unpaired 2 tailed t-test, p=<0.0001, n=5).*

	% of total proteins identified	
	SmN	SmB
Splicing and snRNP assembly	12.1%	9.0%
Methylosome	0.3%	0.2%
Vesicle transport	6.4%	7.4%
Signal transduction	11.7%	11.3%
Neural proteins	2.2%	1.4%
Apoptosis	1.9%	1.8%
Motor Proteins	1.0%	0.7%
Cytoskeletal related proteins	2.8%	1.9%
Mitochondria	3.4%	3.5%
Metabolism and synthesis	12.6%	16.2%
DNA replication and repair	10.8%	10.0%
Transcription	6.5%	6.0%
Post-translation modification	1.9%	3.8%
RNA interacting/processing	7.4%	6.9%
RNA degradation	1.6%	1.5%
Proteolysis	5.0%	5.2%
Unknown	7.8%	5.9%
Other	4.4%	7.3%

C

Sequence	Scaffold Peptide Identification Probability	Mascot Ion Score	Mascot Identity Score	Mascot Delta Ion Score	Observed Mass	Actual Mass	Charge	Δ Dalton	Δ PPM
(R)IFDAVGFTFPNR(L)	100%	45.4	35.1	38.3	692.35	1382.68	2	-0.0140	-10.00
(K)IPILSTFLTAR(G)	100%	56.5	31.7	50.4	616.37	1230.72	2	-0.0150	-12.00
(R)LALEETGTEVK(E)	100%	47.1	36.6	47.1	595.32	1188.62	2	-0.0079	-6.60
(R)LLSTSPALQGTPASR(G)	100%	111.1	34.8	98.9	749.90	1497.79	2	-0.0200	-14.00
(R)LQAGEETASHYR(M)	100%	75.1	34.3	75.1	454.55	1360.63	3	-0.0049	-3.60

969

970 **Figure 2: The interactomes of SmB and SmN are similar, but there are differences present at the level of**
971 **individual proteins**. *A) Immunoblot analysis confirms efficient affinity purification of YFP-SmN, YFP-SmB and*
972 *YFP. 10% of the affinity purified material (left hand lane in each panel) was compared to 80μg of precleared*
973 *lysate (Input) and unbound material using anti-GFP. GFP-Trap effectively immunoprecipitated all three*
974 *proteins. B) After processing the mass spectrometry data, and sorting identified proteins into groups based*
975 *on Gene Ontology annotations, the interactomes of SmN and SmB are very similar. C) Neurochondrin*
976 *(NCDN) was identified in the interactome of YFP-SmN, with 5 unique peptide hits encompassing 9%*
977 *sequence coverage. Each Ion score (Mascot Ion Score) was above the threshold for peptide identity (Mascot*
978 *Identity Score), with 2 out of the 5 identified peptides having a score of above double the threshold score.*

979

980

Figure 3: NCDN interacts with SmN, SmB and SMN, and co-localises with them in vesicles. *A) Affinity isolation of NCDN-GFP using GFP-Trap, detected with anti-GFP (top row) co-enriches mCherry-SmB, detected with anti-mCherry (bottom row) in transiently co-transfected SH-SY5Y cells B) In an SH-SY5Y cell line constitutively expressing NCDN-GFP, affinity isolation of NCDN-GFP, detected with anti-GFP (top row) co-enriches SMN, SmB, SmN and the Coatomer protein βCOP, all detected with antibodies against the endogenous proteins (as labelled). C) In an SH-SY5Y cell line constitutively expressing YFP, affinity isolation of YFP, detected with anti-GFP (top row) does not co-enrich SMN, SmB or βCOP, all detected with antibodies to the endogenous proteins (as labelled). D) in an SH-SY5Y cell line constitutively expressing GFP-SMN, affinity isolation of GFP-SMN, detected with anti-GFP (top row) co-enriches NCDN, detected with anti-NCDN (middle row). Endogenous SMN, detected with anti-SMN (bottom row) is also co-enriched. E) NCDN-GFP and mCherry-SmN co-localise in vesicle-like structures (arrows) in neurites of SH-SY5Y cells constitutively expressing mCherry-SmN, and transiently expressing NCDN-GFP (left hand panels). White areas in the merged image show areas of co-localisation. Co-localisation images (bottom row) were generated in Volocity, using automatic thresholds on undeconvolved z-sections before excluding values below 0.05 (see material and methods). No co-localisation is seen in the same cell line transiently expressing YFP alone (right hand panel). Triangles show structures containing mCherry-SmN, but not YFP. F) mCherry-SMN and NCDN-GFP co-localise in vesicles (arrows) in the cytoplasm of co-transfected SH-SY5Y cells (left hand panels). White areas in the merged image show areas of co-localisation. Co-localisation images (bottom row) were generated as above. No co-localisation is observed between mCherry-SMN and YFP (triangles, right hand panels). Bar= 7μm.*
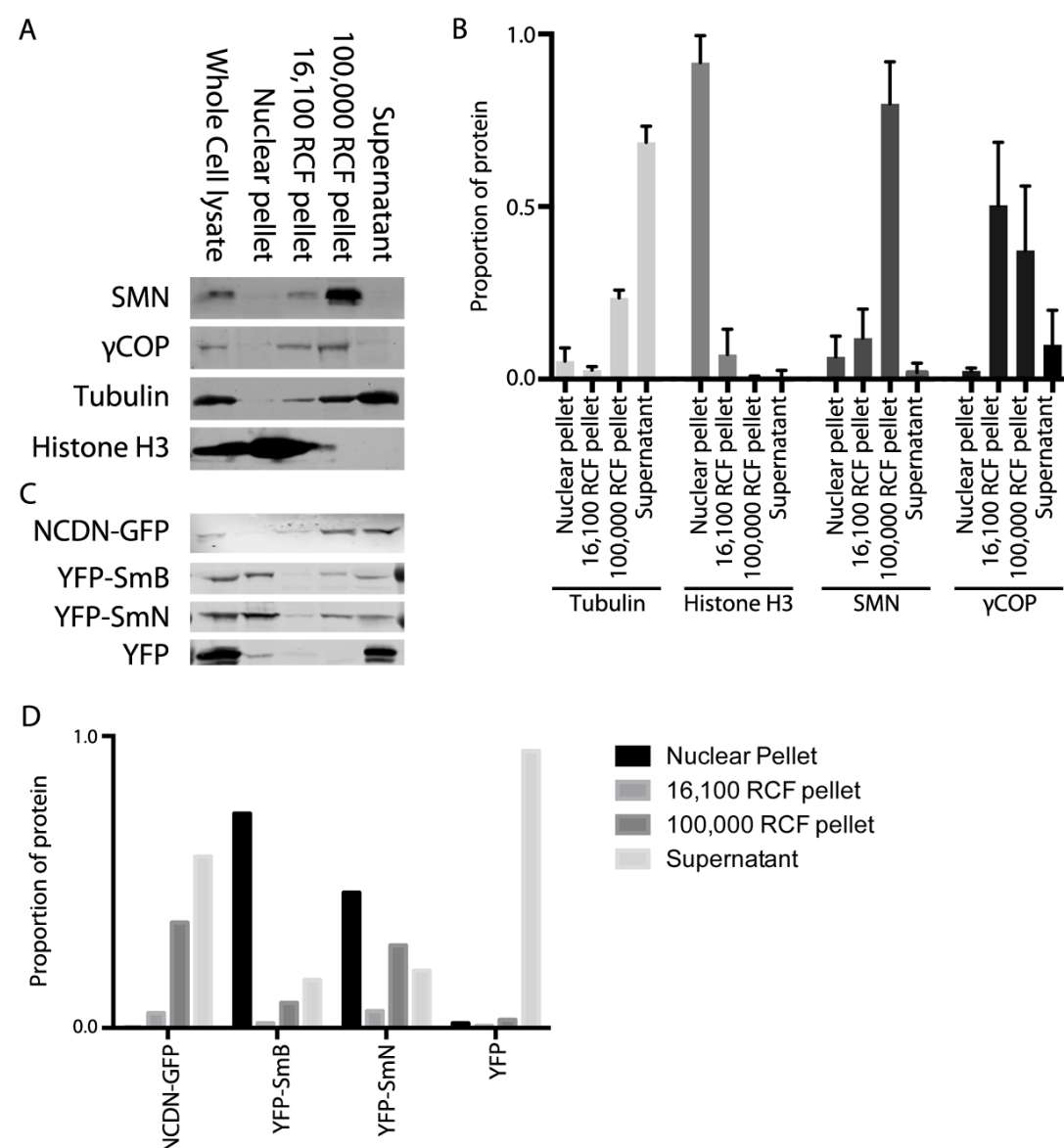
1001

1002

***Figure 4: Detergent-free fractionation of SH-SY5Y cells reveals that SMN, coatomer proteins, NCDN, SmB and SmN are all enriched in the 100,000 RCF vesicle pellet.** A) Immunoblotting of equal protein amounts from fractionated SH-SY5Y cells reveals that SMN (top row) is highly enriched in the 100,000 RCF pellet, with smaller amounts seen in the 16,100 RCF pellet and the nuclear pellet. The coatomer protein, γCOP (second row) is also enriched in the 100,00 RCF pellet as well as the 16,100 RCF pellet. Antibodies to histone H3 and tubulin confirm minimal nuclear contamination in cytoplasmic fractions, and minimal cytoplasmic contamination in the nuclear pellet, respectively. B) Quantitation of immunoblot analysis confirms that SMN is highly enriched in the 100,000 RCF pellet, with enrichment of γCop also seen. Histone H3 and tubulin are highly enriched in the nucleus and cytoplasm respectively. Quantitation of tubulin and histone H3 bands was from 7 immunoblots, with values from SMN and γCOP from 5 and 4 immunoblots respectively. C) Immunoblotting of equal protein amounts from fractionated SH-SY5Y cells constitutively expressing NCDN-GFP, YFP-SmB, YFP-SmN or YFP alone (all detected with anti-GFP) reveals that NCDN-GFP is enriched in the 100,000 RCF pellet, with smaller amounts seen in the 16,100 RCF pellet and the cytosolic supernatant. YFP-SmB and YFP-SmN are both also found in the 100,000 RCF pellet, in addition to the nuclear pellet and cytosolic supernatant. YFP alone is found almost exclusively in the cytosolic supernatant, with none detected in the 100,000 RCF or 16,100 RCF pellets. D) Quantitation of the immunoblots in C) confirms the presence of NCDN-GFP, YFP-SmB and YFP-SmN in the 100,000 RCF pellet, together with the restriction of YFP alone to the residual cytosolic supernatant.*
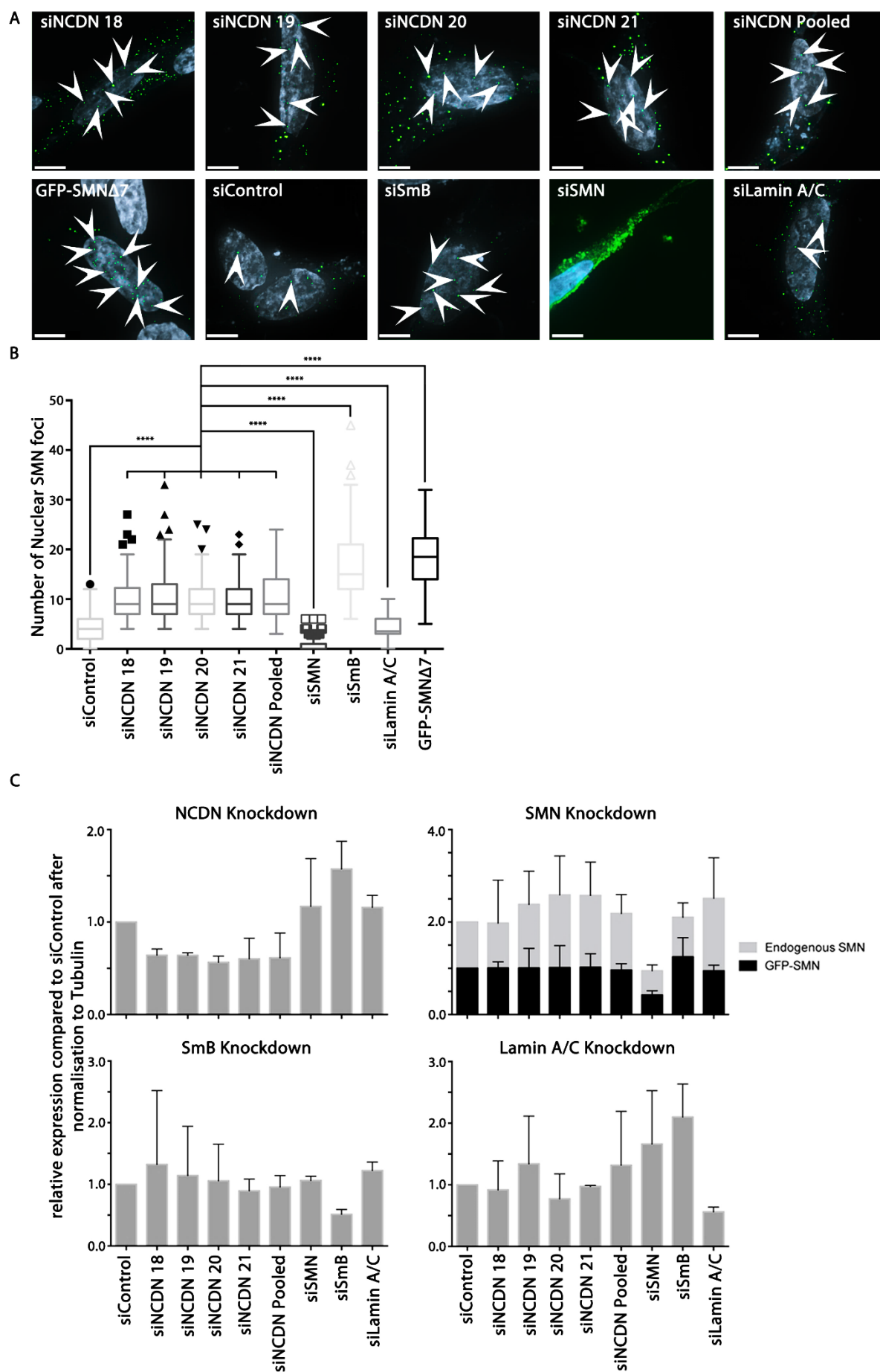
34

1021

1022 **Figure 5: Reduction of endogenous NCDN using siRNA increases localisation of SMN to nuclear gems**. *A)*
1023 *Transfection of SH-SY5Y cells constitutively expressing GFP-SMN (Green) with siRNAs shows an increase in*
1024 *the number of nuclear gems (arrows) in cells transfected with siRNAs against NCDN or SmB and a decrease*
1025 *in the number of nuclear gems in cells transfected with siRNAs against SMN in comparison to cells*
1026 *transfected with non-targeting siRNAs (siControl) or siRNAs against lamin A/C as a' targeting' control.*
1027 *Transfection of SH-SY5Y cells with a plasmid to express GFP-SMNΔ7 also results in increased numbers of*
1028 *nuclear gems. Cell nuclei are stained with Hoescht 33342 (grey on images). Transfection efficiency with*
1029 *siRNAs was greater than 90%, measured by transfection with siGlo Cyclophillin B (not shown). Bar=7μm.*
1030 *Images are deconvolved z-stacks taken with 0.2μm spacing B) Quantitation of numbers of gems per nucleus*
1031 *shows a significant increase following reduction of NCDN (10.2 (± 4.1) with siNCDN 18, 10.4 (± 4.9)) (Mean*
1032 *± Standard Deviation) with siNCDN 19, 9.9 (± 4.1) with siNCDN 20, 9.5 (± 3.6) with siNCDN 21 and 10.7 (±*
1033 *4.6) with siNCDN pooled compared to 4.4 (± 2.5) in cells treated with non-targeting siRNA (siControl) and*
1034 *4.2 (± 2.3) in cells treated with siRNAs targeting lamon A/C (siLaminA/C) . Reduction of SmB also shows an*
1035 *increase in numbers of nuclear gems (to 16.7 (± 6.8) with siSmB), while reduction of SMN leads to a*
1036 *decrease in numbers of nuclear gems (to 0.7 (± 1.4) with siSMN). Expression of GFP-SMNΔ7 results in an*
1037 *increase of numbers of nuclear gems to 18.2 (± 5.3). The difference between each siNCDN and controls is*
1038 *statistically significant (AVOVA; P<0.0001, n=150 from 3 replicates). A Tukey post-test identified outliers*
1039 *(individual points marked on graph). C) Immunoblot analysis using antibodies to endogenous NCDN, SMN*
1040 *and SmB shows a reduction in expression of each of 40-60% compared to siControl cells, after signals were*
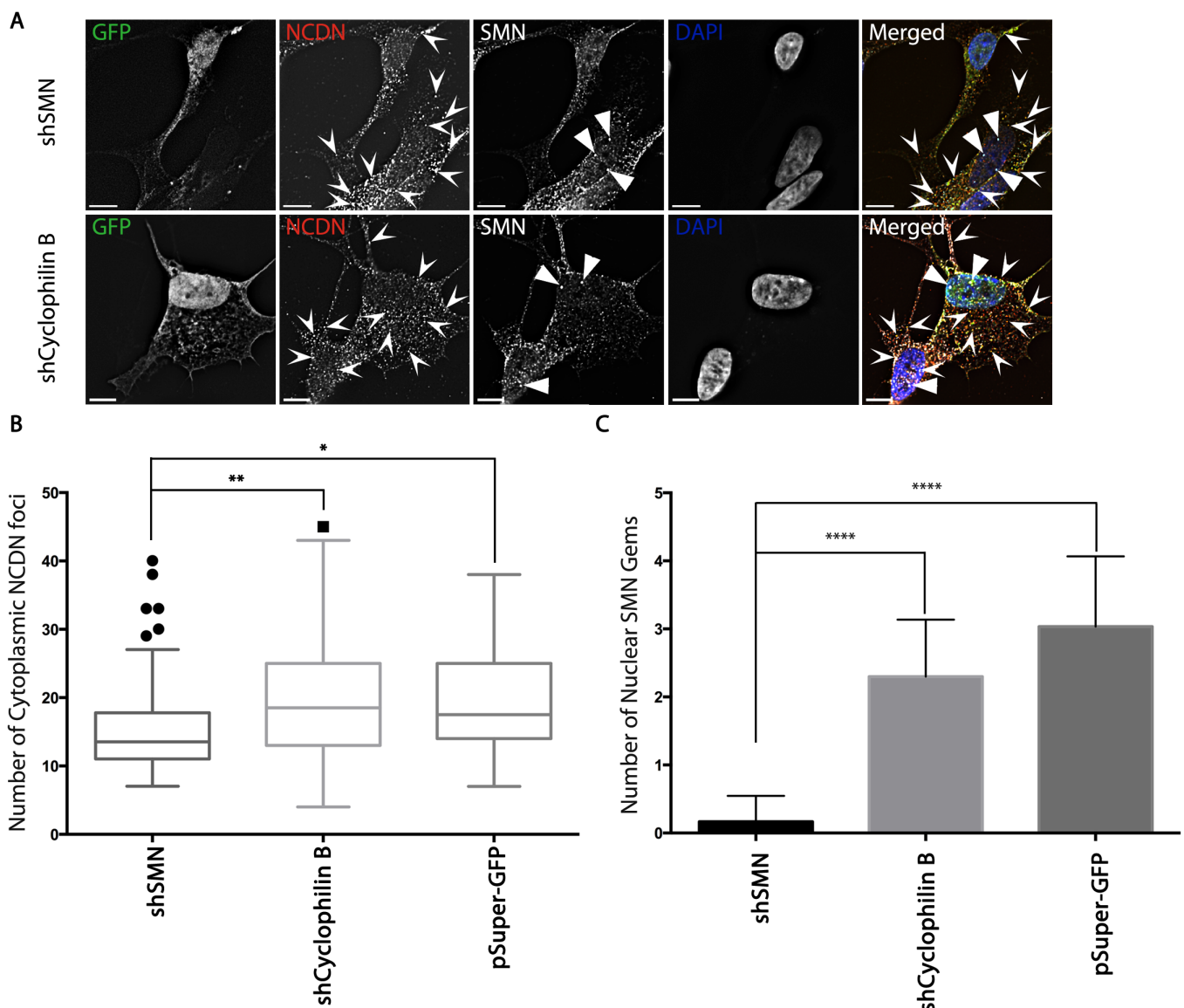1041 *normalised to tubulin.*

1042

Figure 6: Reduction of endogenous SMN causes a reduction in cytoplasmic NCDN foci in SH-SY5Y cells. A)
SH-SY5Y cells were transfected with plasmids to express shRNAs targeting SMN (shSMN), Cyclophilin B
(shCyclophilin) or with the empty pSuper GFP vector (not shown) were fixed after 72 hours, and
immunostained for endogenous NCDN and SMN, allowing detection of NCDN foci within the cytoplasm of
the cells (identified with Arrowheads), as well as SMN-positive nuclear Gems (identified with Triangles).
Bar= 7μm, images are single deconvolved z-sections B) The depletion of SMN results in a reduction in the
number of NCDN foci present in the cytoplasm to 15.3 (± 7.2) (Mean ± Standard Deviation) from 20.6 (±
12.0) and 19.5 (± 7.6) compared to cells either transfected with shCyclophilin B or the empty pSuper GFP
vector respectively (ANOVA P<0.0005, n=64 from 3 replicates). C) The depletion of SMN causes a reduction
of nuclear Gems to 0.17 (± 0.38) from 2.3 (± 0.84) or 3.0 (± 1.0) compared to cells transfected with
shCyclophilin B or empty vector respectively (ANOVA P<0.0001, n=30 from 3 replicate).
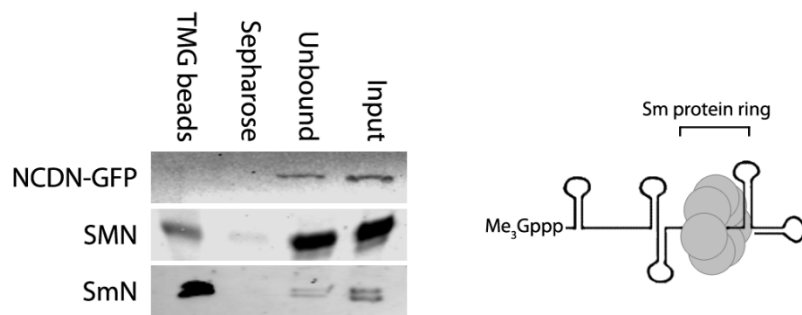
1054

Figure 7: NCDN-GFP does not co-purify with snRNPs in SH-SY5Y cells constitutively expressing NCDN-GFP. *Incubation of whole-cell lysate from an SH-SY5Y cell line constitutively expressing NCDN-GFP with agarose beads conjugated to antibodies against the tri-methyl guanosine cap (Me3Gppp) of snRNAs (TMG beads) affinity purifies snRNPs as evidenced by the enrichment of the core snRNP protein SmN (detected with anti-SmN, bottom row). The enriched snRNP fraction also contains SMN, which is essential for snRNP assembly. NCDN-GFP,however, does not co-enrich with snRNPs. Also shown is the core structure of mature snRNPs consisting of the heptameric Sm protein ring bound at the Sm binding site of snRNA, as well as the characteristic tri-methyl guanosine Cap of snRNAs (Me$_3$Gppp) at the 5' end.*
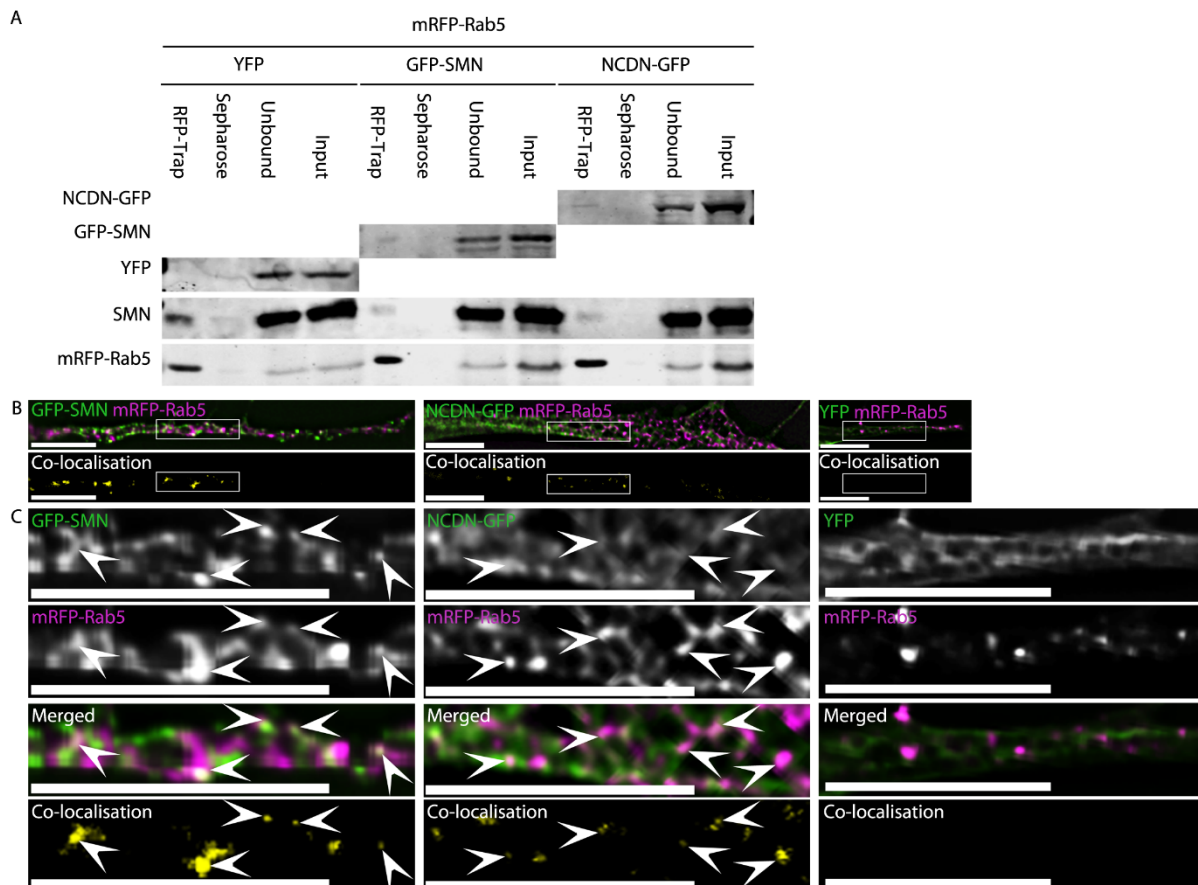
1063

1064

Figure 8: NCDN and SMN interact with Rab5 and co-localise with a subset of Rab5 vesicles within neurites of SH-SY5Y cells. A) Affinity isolation of mRFP-Rab5 using RFP-Trap from cells co-transfected with plasmids to express mRFP-Rab5 together with NCDN-GFP, GFP-SMN or YFP alone co-enriches both NCDN-GFP (top row, detected with anti-GFP, band is present in RFP-Trap lane but not sepharose beads lane) and SMN-GFP (second row, detected with anti-GFP, band is present in RFP-Trap lane but not sepharose beads lane), but not YFP (third row, no band detected in RFP-Trap lane). Endogenous SMN (fourth row, detected with mouse anti-SMN) co-enriches with mRFP-Rab5 in all three samples. Detection of mRFP-Rab5 (bottom row, detected with anti-RFP) confirms robust enrichment of mRFP-Rab5 in all three samples. B) Both GFP-SMN and NCDN-GFP partially co-localise with mRFP-Rab5 in a subset of mRFP-Rab5 containing vesicles in co-transfected SH-SY5Y cells (white signal in overlaid images, top row; yellow signal in co-localisation images, bottom row). C) Enlargement of the boxed areas in B confirm that the co-localisation between SMN/NCDN and Rab5 occurs in punctate structures. Arrowheads identify areas of co-localisation. Co-localisation images were generated by Volocity, using automatic thresholds on non-deconvolved z-sections before excluding values below 0.05. Images (excluding the co-localisation images) are single deconvolved z-sections. Bar=7μm.
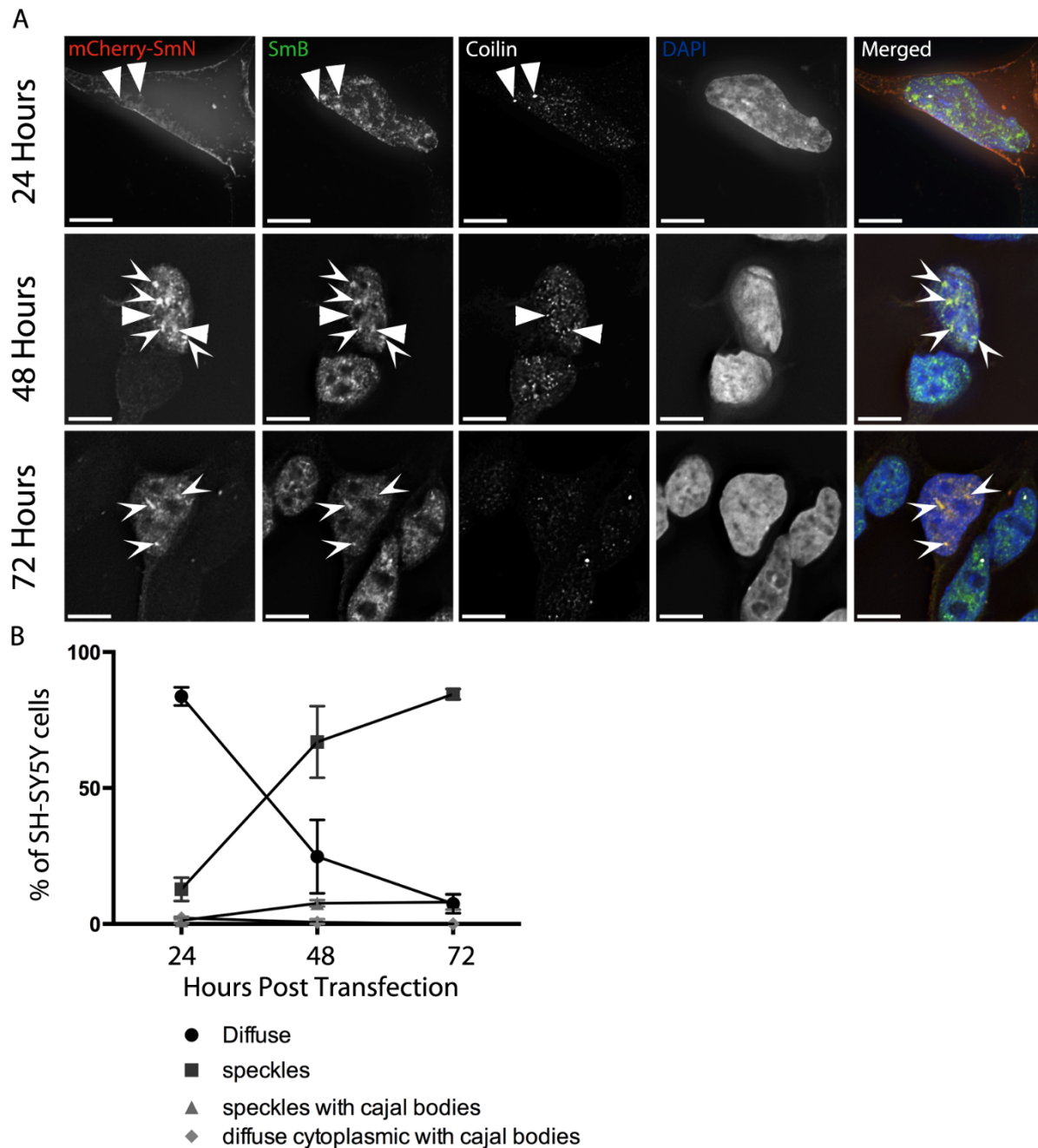
1079

1080 *Figure S1: mCherry-SmN exhibits similar behaviour to both YFP-SmN and SmB in SH-SY5Y cells. A) SH-SY5Y*
1081 *cells transiently expressing mCherry-SmN and fixed after 24, 48 and 72 hours show variations in distribution*
1082 *of the mCherry-SmN with time. Immunostaining with Y12 (green on overlay) and anti-coilin (white on*
1083 *overlay) shows splicing speckles (arrowheads) and Cajal Bodies (CBs, triangles) respectively. Images are*
1084 *deconvolved z-stacks with 0.2 μm spacing. Bar=7μm. B) mCherry-SmN initially localises diffusely in the*
1085 *cytoplasm, before localising to speckles at the 48 and 72 hour time-points. 3 independent experiments,*
1086 *n=100 cells per experiment. Data shown is mean ± SD.*

1087

Identified protein	Accession number	Molecular Weight	SmN	SmB	YFP
small nuclear ribonucleoprotein polypeptide B * [Homo sapiens]	gi|53690154	24 kDa	13	11	2
small nuclear ribonucleoprotein Sm D2 isoform 1 [Homo sapiens]	gi|4759158	14 kDa	10	8	4
small nuclear ribonucleoprotein Sm D1 [Homo sapiens]	gi|5902102	13 kDa	5	5	4
small nuclear ribonucleoprotein E [Homo sapiens]	gi|4507129	11 kDa	5	4	2
small nuclear ribonucleoprotein F [Homo sapiens]	gi|4507131	10 kDa	5	3	0
small nuclear ribonucleoprotein Sm D3 [Homo sapiens]	gi|4759160	14 kDa	4	4	3
small nuclear ribonucleoprotein G [Homo sapiens]	gi|4507133	8 kDa	4	3	0
survival motor neuron protein isoform a [Homo sapiens]	gi|13259527	30 kDa	8	7	0
GEMIN5 protein [Homo sapiens]	gi|219517971	168 kDa	22	25	0
HC56 (Gemin 4) [Homo sapiens]	gi|10945430	119 kDa	18	11	0
DEAD box RNA helicase Gemin3 [Homo sapiens]	gi|6503002	92 kDa	12	18	0
gem-associated protein 2 isoform alpha [Homo sapiens]	gi|4506961	32 kDa	6	4	0
gem-associated protein 8 [Homo sapiens]	gi|8923481	29 kDa	6	2	0
Gem (nuclear organelle) associated protein 6 [Homo sapiens]	gi|17390437	19 kDa	3	3	0
gem-associated protein 7 [Homo sapiens]	gi|13376001	15 kDa	3	2	0
WD-40 repeat protein (Unrip) [Homo sapiens]	gi|4519417	38 kDa	16	16	0
U6 snRNA-associated Sm-like protein LSm4 isoform 1 [Homo sapiens]	gi|6912486	15 kDa	5	4	0
U6 snRNA-associated Sm-like protein LSm2 [Homo sapiens]	gi|10863977	11 kDa	4	4	0
U6 snRNA-associated Sm-like protein LSm6 [Homo sapiens]	gi|5901998	9 kDa	2	2	0
U6 snRNA-associated Sm-like protein LSm3 [Homo sapiens]	gi|7657315	12 kDa	2	2	0
U6 snRNA-associated Sm-like protein LSm7 [Homo sapiens]	gi|7706423	12 kDa	2	0	0
U7 snRNA-associated Sm-like protein LSm11 [Homo sapiens]	gi|27735089	40 kDa	2	0	0
protein arginine N-methyltransferase 5 isoform a [Homo sapiens]	gi|20070220	73 kDa	30	31	3
methylosome protein 50 [Homo sapiens]	gi|13129110	37 kDa	12	10	0
methylosome subunit pICln [Homo sapiens]	gi|4502891	26 kDa	7	8	0
CD2 antigen cytoplasmic tail-binding protein 2 [Homo sapiens]	gi|5174409	38 kDa	13	12	0
PERQ amino acid-rich with GYF domain-containing protein 2 isoform c [Homo sapiens]	gi|156766047	149 kDa	2	4	0
WW domain-binding protein 4 [Homo sapiens]	gi|6005948	43 kDa	3	0	0
formin binding protein 4, isoform CRA_a [Homo sapiens]	gi|119588290	90 kDa	2	2	0
neurochondrin isoform 2 [Homo sapiens]	gi|62526031	79 kDa	5	0	0
nuclear receptor coactivator 6 interacting protein, isoform CRA_b [Homo sapiens]	gi|119607168	97 kDa	13	0	0
7SK snRNA methylphosphate capping enzyme isoform A [Homo sapiens]	gi|47271406	74 kDa	13	0	0
RNA-binding protein 40 [Homo sapiens]	gi|40538732	59 kDa	13	0	0

Table S2: A selected dataset from the interactome analysis of SmN and SmB confirms efficient identification of known Sm protein interactors. All other core Sm family proteins were identified in the interactome analysis, as well as SMN, all Gemin components of the SMN complex and several LSm proteins, including LSm11 (found only in the U7 snRNP). Additionally, several members of the methylosome, where SmB post-translational modifications occur, were identified including Protein arginine N-methyltransferase 5 (PRMT5). Several previously identified SmB interactors (CD2 antigen cytoplasmic tail binding protein-2, PERQ2, WW domain-binding protein 4 and Formin binding protein 4) (Bedford et al. 1998, Bedford et al. 2000, Kofler et al. 2004, Kofler et al. 2005) were identified to interact with at least one of the proteins. * denotes that spectra from SmN were pooled with those from SmB by Scaffold due to sequence similarity in the majority of the proteins. Neurochondrin, and other proteins discussed are also shown here. Values are number of unique peptides identified.
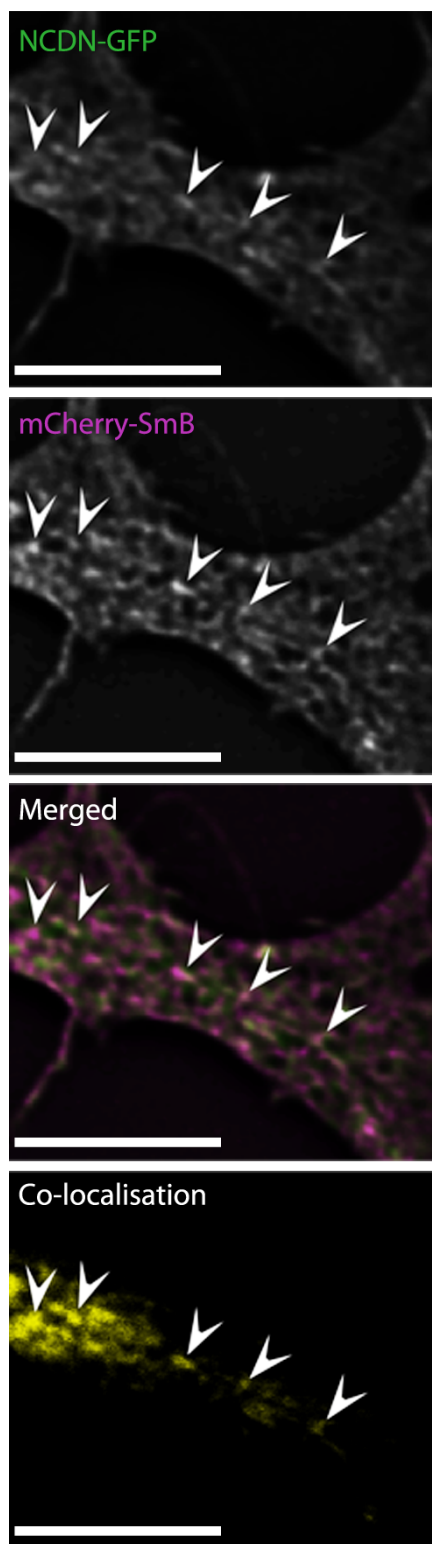
1102

1103   *Figure S3: NCDN and SmB co-localise in neurites of SH-SY5Y cells constitutively expressing mCherry-SmB,*
1104   *and transiently expressing NCDN-GFP. Arrows identify SmB containing-vesicles with NCDN co-localisation.*
1105   *Bar= 7μm, images are single deconvolved z-sections. Co-localisation images were generated by Volocity,*
1106   *using automatic thresholds on undeconvolved z-sections (see materials and methods).*
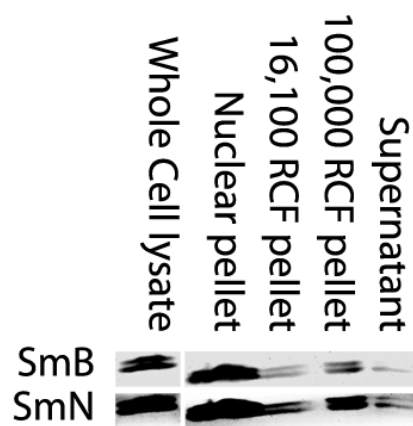
1107

Figure S4: Endogenous SmB and SmN fractionate similarly to YFP-SmB and YFP-SmN, with both present in the 100,000 RCF vesicle fraction in addition to being highly enriched in the nuclear pellet of fractionated SH-SY5Y cells. The gap between bands in the whole cell lysate and cell fractions signifies omitted lanes.

Movie S1: punctate structures containing mCherry-SmN are mobile structures within the cytoplasm of SH-SH5Y cells. Images were taken every ~2 seconds for ~150 seconds. Movie is a projection of 3 deconvolved z-stacks taken with 0.5μm spacing. Bar=7μm.